

# Diffusion shocks in an inhomogeneous current-carrying collisional plasma

A. P. Dmitriev, V. A. Rozhanskii, and L. D. Tsandin

*A. F. Ioffe Physicotechnical Institute, Academy of Sciences of the USSR, Leningrad*

*M. I. Kalinin Polytechnic Institute, Leningrad*

*Usp. Fiz. Nauk* **146**, 237–265 (June 1985)

The evolution of density profiles in current-carrying inhomogeneous plasma is examined for evolution rates that are slow in comparison with acoustic and Alfvén velocities. When the density profile is smooth in comparison with  $l_T = T/eE$ , diffusion is initially unimportant and evolution can often be described by the equation for a simple nonlinear wave. The breaking of this wave leads to the appearance of regions with a steep density gradient, i.e., diffusion shocks. The exception is ambipolar diffusion in simple plasma consisting of ions and electrons of a single kind and having constant mobilities. Examples of such stationary and moving shocks in ionospheric, gas-discharge, and semiconductor plasmas, and in electrolytes, are discussed.

## CONTENTS

1. Introduction.....	467
2. Weakly ionized multicomponent plasma in the absence of a magnetic field.....	469
A. Three-component plasma with one kind of fixed ions. B. Structure of diffusion shock. C. Three-dimensional case. D. Three-component plasma with constant mobilities. E. Formation of shocks in gas-discharge plasma.	
3. Evolution of shocks in initial conditions.....	472
4. Weakly-ionized plasma in a magnetic field.....	473
A. One-dimensional case. B. Shocks in the Hall direction. C. Effect of ionization and recombination on the evolution of shocks.	
5. Partially and fully ionized plasma.....	476
A. Partially ionized plasma in a magnetic field. B. Fully ionized plasma in zero magnetic field. C. Fully ionized plasma in a magnetic field.	
6. Diffusion shocks in semiconductor plasma.....	478
A. Evolution of the profile as carriers heat up in a semiconductor with fully ionized donors. B. Stationary profiles with shocks. C. Shocks in a semiconductor with carriers captured by traps. D. Structure of a shock in a specimen containing traps. Relaxation zone.	
7. Conclusion .....	482
References.....	482

## 1. INTRODUCTION

Problems involving the shape and evolution of spatially-inhomogeneous charged-particle density distributions in the presence of a current flowing through the system are frequently encountered in different branches of physics. Such problems are very topical in the physics of semiconductors, gas discharges, and electrolytes. Similar problems arise in the analysis of the motion of inhomogeneities in ionospheric and fully ionized plasmas.

If we confine our attention to isothermal plasmas, the evolution of the inhomogeneous plasmas is determined by the particle mobility and diffusion, and is commonly described by the following set of equations:

$$\frac{\partial n_\alpha}{\partial t} + \operatorname{div} \Gamma_\alpha^{(t)} = I_\alpha - R_\alpha, \quad (1.1)$$

$$\Gamma_\alpha^{(t)} = \frac{Z_\alpha}{|Z_\alpha|} \hat{b}_\alpha n_\alpha \mathbf{E} - \hat{D}_\alpha \nabla n_\alpha, \quad \alpha = 1, 2, \dots, k; \quad (1.2)$$

where  $Z_\alpha$  is the charge on particles of type  $\alpha$  and  $\hat{D}_\alpha, \hat{b}_\alpha$  are the diffusion and mobility coefficients (which are tensors in a magnetic field or in anisotropic media). We shall consider that the Einstein relation

$$\hat{D}_\alpha = \frac{T_\alpha}{e |Z_\alpha|} \hat{b}_\alpha \quad (1.3)$$

is satisfied. The terms  $I_\alpha, R_\alpha$  correspond to the generation and recombination of particles. The quasineutrality conditions

$$\sum_\alpha Z_\alpha n_\alpha = 0, \quad \sum_\alpha Z_\alpha (I_\alpha - R_\alpha) = 0 \quad (1.4)$$

determine the self-consistent electric field in the system.

For the so-called simple plasma without a magnetic field, which contains only two types of carrier whose mobilities do not depend on the density, field, or direction, the set of equations given by (1.1)–(1.4) reduces to the well-known ambipolar diffusion equation<sup>1</sup>

$$\frac{\partial n_{1,2}}{\partial t} - D_a \Delta n_{1,2} = I_{1,2} - R_{1,2}, \quad (1.5)$$

where  $D_a = (b_1 D_2 + b_2 D_1)/(b_1 + b_2)$  is the ambipolar diffusion coefficient. This linear equation does not contain the electric field, so that the evolution of the plasma inhomogeneity is independent of the current. This situation is, however, exceptional. Even in the absence of a current in a system consisting of more than two kinds of carrier with

constant mobilities (for example, electrons and two kinds of ion in weakly ionized plasmas, or electrons, holes, and fixed charged centers in semiconductors), the system defined by (1.1)–(1.4) can no longer be reduced to the ambipolar diffusion equation. In particular, at certain stages of the evolution process, the field fluxes can collect some of the components at their density maxima. For example, in a gas discharge, the ambipolar field confines electrons to the plasma. Since, usually,  $T_e \gg T_i$ , negative ions are drawn by this field into the plasma in the case of electronegative gases, thus producing sharply inhomogeneous profiles detached from the wall.<sup>2</sup> In the general case, the diffusive evolution of inhomogeneities in multicomponent plasmas is a relatively complex process that depends on the shape of the initial inhomogeneity and on the degree of nonlinearity, i.e., on the relative drop in the component densities. The situation is simplified in the linear case, when density perturbations are small in comparison with the stationary homogeneous background. The general solution of the linearized system (1.1)–(1.4) consists of the sum of  $k - 1$  diffusion modes  $\omega_q = \omega_q(k^2)$ , each of which in general depends on the diffusion coefficients of all the components and on the generation-recombination terms in (1.1). The transition to ambipolar diffusion was investigated in Refs. 3 and 4 by considering the example of three-component plasma in which the mobilities of the two kinds of positive ion were equal. It was found that the linearity of (1.5) was a consequence of the complete mutual compensation of several nonlinear effects.

The nature of the evolution of an inhomogeneity is, in general, radically altered when a sufficiently strong current is introduced into the system. One can then arbitrarily identify two groups of effects. Firstly, there are the effects associated with the change in the rates of generation-recombination processes in the electric field due to the plasma inhomogeneity. They include, for example, losses,<sup>5,6</sup> several instabilities in the gas discharge,<sup>7,8</sup> many phenomena near the electrodes, and so on. We shall not touch upon these complicated and interesting problems, and will confine our attention to the analysis of the effect of the self-consistent electric field of the inhomogeneity on its evolution, which is due to the change in the diffusion and field fluxes (1.2). The characteristic feature of the resulting density profile is the steepening of the inhomogeneities, i.e., the appearance of regions in which the density gradients of the components can substantially exceed the initial values. The reason for this phenomenon is as follows. For sufficiently smooth inhomogeneities, whose characteristic scale in the direction of the current is  $L \gg l_T = T/eE$ , the diffusion terms can be neglected in the fluxes (1.2). When generation and recombination are unimportant, which is frequently referred to as the drift approximation,<sup>9</sup> the linearized system (1.1)–(1.4) describes the propagation of  $(k - 1)$  different types of undamped wave.<sup>1)</sup> The nonlinearity of the finite-amplitude waves is reflected, above all, in the fact that different points on the wave profile move with different velocities. This results in wave breaking, i.e., the density profile becomes multivalued in the drift approximation. To obtain physically meaningful results, we must take into account the diffusion

components of the fluxes (1.2). Diffusion arrests wave breaking, and narrow regions (of width  $\sim l_T$ ) in which the plasma parameters are subject to rapid variation are found to appear. For waves of small amplitude, the problem can be reduced to the Burgers equation.<sup>13</sup> These diffusion shocks are analogous to shock waves in ordinary gas dynamics.<sup>13–14</sup> As in the latter case, they may be looked upon as discontinuities in drift velocities, where the position and velocity of these discontinuities can be found without investigating the diffusion processes. Diffusion determines only the density profile in the interior of the shock. The influence of generation and recombination can frequently be reduced to the broadening of the shock and to a complication of its structure, namely, the formation of a relaxation zone, as in the propagation of a shock wave in a relaxing gas.<sup>14–15</sup>

Kolrausch and Weber<sup>16,17</sup> were the first to note the formation of shocks in electrolytes. They showed that, in a fully dissociated electrolyte containing three types of ion, the flow of current produced discontinuities in drift solutions. If ion mobility depends on ion density, these discontinuities should also occur in the solution containing two kinds of ion. Laue<sup>18</sup> has generalized these results to the case of a variable degree of dissociation. Particular attention was devoted in these papers and in experiments<sup>19–21</sup> to the evolution of an arbitrary discontinuity in initial conditions. It was shown that, depending on the direction of the current in the electrolyte containing two kinds of ion, the mobility of which depends on density, the boundary between solutions with different concentration can move, remaining sharp, or it can diffuse. On the other hand, when there are three kinds of ion, the sharp boundary may split into two discontinuities in the course of the evolution process, namely, a moving and a stationary discontinuity.<sup>17</sup> When the current is reversed, a continuous density profile and one stationary discontinuity are produced. The structure of a weak discontinuity was examined in Ref. 20, where an expression analogous to the formula for the profile of a weak shock wave<sup>13–15</sup> was obtained. The corresponding measurements were found to be in good agreement with theory.

A. V. Gurevich,<sup>22</sup> who considered the example of partially ionized plasma in a magnetic field, was probably the first to note the formation of diffusion shocks. The nonlinearity of (1.1)–(1.4), which leads to the breaking of the drift profile, was due to the dependence of the transport coefficients on the charged-particle densities, which in turn was due to Coulomb collisions.

Sharply inhomogeneous density and field profiles have been observed<sup>23,24</sup> in semiconductors with hot carriers. It was noted in Refs. 25–27 that they constituted stationary diffusion shocks, produced because the electron mobility was a function of the electric field. Numerical simulation of the evolution of inhomogeneities in ionospheric plasmas led to the discovery<sup>28</sup> of regions in which there was a sharp rise in the density gradient. These regions can be interpreted as diffusion shocks.<sup>29,30</sup> It is shown in Refs. 30 and 31 that the generation-recombination terms in (1) frequently lead to the broadening of the shocks and to the formation of a relaxation zone.

Since Eqs. (1.1)–(1.4) have a wide range of validity, the formation of such diffusion shocks is a relatively general feature of current-carrying plasmas. Factors such as the multi-component nature of the plasma, Coulomb collisions, dependence of mobility on electric field, anisotropy produced by a magnetic field, and plasma inhomogeneity across the field, lead to nonlinear equations, when the quasineutrality condition is taken into account, and to the breaking of the drift profiles. Hence, the corresponding sharply inhomogeneous distribution of charged-particle density and electric field appear under very different conditions during the evolution of inhomogeneities in gas-discharges, ionospheric and semiconductor plasmas, and electrolytes and fully ionized plasmas.

The steepening of density profiles in current-carrying plasmas may be the reason, especially in a magnetic field, for the numerous instabilities seen experimentally. These are complicated phenomena that have not been well studied. In the first instance, they appear as a broadening and turbulization of the shock itself. We shall not examine these questions except when direct experimental evidence is available.

We shall consider several examples which we will use to illustrate the characteristic features of this phenomenon.

## 2. WEAKLY IONIZED MULTICOMPONENT PLASMA IN THE ABSENCE OF A MAGNETIC FIELD

Consider a plasma containing electrons and two kinds of positive ion. Let  $I_\alpha = R_\alpha = 0$  and suppose that the  $b_\alpha$  are constants. Neglecting diffusion, and using the quasineutrality condition

$$n_e = n_1 + n_2, \quad (2.1)$$

we find that, in the one-dimensional case,

$$E = E_0 \frac{(b_1 + b_e) n_1^{(0)} + (b_2 + b_e) n_2^{(0)}}{(b_1 + b_e) n_1 + (b_2 + b_e) n_2} = \frac{j/e}{(b_1 + b_e) n_1 + (b_2 + b_e) n_2}, \quad (2.2)$$

$$\frac{\partial n_\alpha}{\partial t} + b_\alpha E_0 [(b_1 + b_e) n_1^{(0)} + (b_2 + b_e) n_2^{(0)}] - \frac{\partial}{\partial x} \frac{n_\alpha}{(b_1 + b_e) n_1 + (b_2 + b_e) n_2} = 0, \quad \alpha = 1, 2, \quad (2.3)$$

where  $E_0$ ,  $n_\alpha^{(0)}$  are, respectively, the field and density of the uniform-plasma components at infinity.<sup>2)</sup>

### A. Three-component plasma with one kind fixed ions

The simplest case is  $b_e \gg b_1, b_2 = 0$ .<sup>3)</sup> We then have  $n_2 = n_2^{(0)} = \text{const}$ , so that (2.3) yields

$$\frac{\partial n_1}{\partial t} + V(n_1) \frac{\partial n_1}{\partial x} = 0, \quad (2.4)$$

where the velocity of points on the profile  $V(n_1)$  is the nonlinear analog of the rate of ambipolar drift, which is related to the flux in the drift approximation,  $\Gamma_1(n_1)$ :

$$V(n_1) = \frac{d\Gamma_1(n_1)}{dn_1} = \frac{j b_1 n_2^{(0)}}{e b_e (n_1 + n_2^{(0)})^2}. \quad (2.5)$$

The solution of (2.4) is<sup>13)</sup>

$$n_1(x, t) = n_{10}(x - V(n_1)t), \quad (2.6)$$

where  $n_{10}(x)$  is the initial density profile of ions of kind 1.

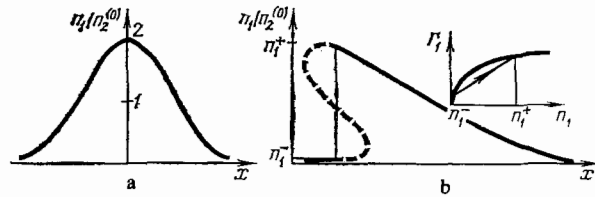


FIG. 1. a—Initial density profile,  $n_1$ ; b— $n_1$  profile for  $t > t_c$ ,  $A = 2$ . Insert shows a graph of  $\Gamma_1(n_1)$ .

Consider the evolution of the simple initial Gaussian profile  $n_{10}(x,0) = An_2^{(0)} \exp(-x^2/a^2)$  (Fig. 1a). It is clear from (2.5) that  $V(n_1)$  decreases with increasing  $n_1$ , i.e., points corresponding to greater density move more slowly. The result is that the frontside of the profile becomes flatter, whereas the backside steepens and then becomes multivalued, so that the wave breaks. Since wave breaking produces a sharp rise in the density gradient, diffusion becomes important in a narrow region. The onset of the shock can be defined by<sup>13–15)</sup>

$$t_c = \min \left[ \frac{dV(n_1(x))}{dx} \right]^{-1}, \quad (2.7)$$

i.e., the instant of time at which the characteristics (2.4) begin to cross in the  $(t,x)$  plane. The position of the shock and the concentrations  $n_1^-$  and  $n_1^+$  on the left and right of the shock can be determined readily from the conservation of the number of particles, since the area under the curve  $n_1(x)$  with the shock should be equal to the area under the three-valued drift solution (Fig. 1b);  $n_1^+ > n_1^-$ . The shock velocity  $W$  can be determined from the conservation of flux in the coordinate frame attached to the shock.

$$W = \frac{\Gamma_1(n_1^+) - \Gamma_1(n_1^-)}{n_1^+ - n_1^-}. \quad (2.8)$$

### B. Structure of a diffusion shock

When diffusion is taken into account, instead of (2.4) we have

$$\frac{\partial n_1}{\partial t} + \frac{\partial \Gamma_1}{\partial x} - \frac{\partial}{\partial x} \left[ D_a(n_1) \frac{\partial n_1}{\partial x} \right] = 0, \quad (2.9)$$

where  $D_a \simeq D_1(2n_1 + n_2^{(0)})/(n_1 + n_2^{(0)})$  is the ambipolar diffusion coefficient for  $b_e \gg b_1$ . Transforming to the coordinate frame moving with the shock velocity  $W$ , and neglecting the slow variation of  $W$  with time, we obtain

$$-W \frac{dn_1}{dX} + \frac{d\Gamma_1}{dX} - \frac{d}{dX} \left[ D_a(n_1) \frac{dn_1}{dX} \right] = 0, \quad (2.10)$$

where  $X = x - Wt$ . This equation has a solution that tends asymptotically to  $n_1^\pm$  for  $X \rightarrow \pm \infty$  if  $W$  is given by (2.8) and  $n_1^+ > n_1^-$ . Integrating (2.10), we obtain

$$\frac{dn_1}{dX} = \frac{j}{b_e T} \frac{(n_1^+ - n_1)(n_1 - n_1^-) n_2^{(0)}}{(2n_1 + n_2^{(0)})(n_1^+ + n_2^{(0)})(n_1^- + n_2^{(0)})}, \quad (2.11)$$

which determines the density profile in the shock. The spatial scale of a strong shock ( $n_1^+ - n_1^- \gtrsim n_2^{(0)}$ ) is  $\sqrt{l_T^+ l_T^-}$  ( $l_T^\pm$  are the values of  $l_T = T/eE$  to the left and right of the discontinuity), and the potential drop across it is  $\sim T/e$ . For a weak shock ( $\Delta n_1 = n_1^+ - n_1^- \ll n_2^{(0)}$ ), it follows from (2.11)

$$n_1(X) = \frac{n_1^+ - n_1^-}{2} \operatorname{th} \frac{X(n_1^+ - n_1^-)n_2^{(0)}}{2l_T(n_1^+ + n_2^{(0)})(2n_1^+ + n_2^{(0)})} + \frac{1}{2}(n_1^+ + n_1^-), \quad (2.12)$$

and the shock width is proportional to  $(\Delta n_1)^{-1}$  (Refs. 13–15).

When the plasma density is low enough, the Debye length  $r_d$  becomes greater than  $l_T$ . The quasineutrality condition is then violated in the shock, and its width becomes of the order of  $l_0 = r_d^2 l_T \gg r_d, l_T$ . The potential drop across it is much greater than  $T/e$ , and this may be looked upon as an analog of the double layer in plasmas with collisions.<sup>55</sup> As in gas dynamics, the evolution of the drift profile (2.6) and the position and velocity of the shocks (2.8) are independent of structure. We shall assume through out that  $l_T$  (or  $l_0$ ) are small in comparison with the characteristic scales of the problem. Thus, if the initial density profile  $n_{10}(x)$  has a discontinuity, then, for  $n_1^+ > n_1^-$ , the discontinuity will propagate with velocity (2.8) without spreading out by diffusion. In the opposite case, on the other hand, the characteristics of (2.4) on the  $(x, t)$  plane are found to fan out,<sup>13–15</sup> so that the discontinuity with  $n_1^+ < n_1^-$  vanishes. It is commonly said that this discontinuity does not satisfy the evolution condition.<sup>32–33</sup> It is then convenient to use the graph of the drift flux  $\Gamma_1(n_1)$  (see Fig. 1b) which, in our case, plays the same role as the well-known Hugoniot adiabat in gas dynamics. The directed segment  $(n_1^- \rightarrow n_1^+)$  on the  $\Gamma_1(n_1)$  graph corresponds to the diffusion shock. According to (2.8), its slope is equal to the velocity of the shock. The arrow shows that the density in the shock satisfying the evolution condition must increase. In fact, the total flux in the shock is lower than the drift flux, i.e., the diffusion flux must be negative ( $n_1^- < n_1^+$ ). In general, the shock is stable<sup>14,32</sup> if the velocity of small signals on either side of it is directed toward the shock, i.e.,

$$V(n_1^-) > W_1^- > V(n_1^+). \quad (2.13)$$

Since the graph of  $\Gamma_1(n_1)$  is convex, it follows that  $n_1^- < n_1^+$ .<sup>4</sup>

The evolution of a complex initial profile may lead to the appearance of several discontinuities, their coalescence, and so on. Asymptotically, for  $|n_1/n_1^{(0)} - 1| \ll 1$ , an arbitrary perturbation will, in general, transform into a rectangular wave with a diffusion shock on the backside for  $n_1 > n_1^{(0)}$  and on the frontside for  $n_1 < n_1^{(0)}$  (Ref. 13).

### C. Three-dimensional case

Instead of (2.4), we have

$$\frac{\partial n_1}{\partial t} + \operatorname{div} \frac{b_1 n_1 \mathbf{j}}{e b_e (n_1 + n_2^{(0)})} = 0, \quad (2.14)$$

where the current density is  $\mathbf{j} = e b_e (n_1 + n_2^{(0)}) \mathbf{E}$  and satisfies the equation

$$\operatorname{div} \mathbf{j} = 0. \quad (2.15)$$

We now introduce the coordinates  $\zeta, \xi$ , which label the current lines, and the coordinate  $\lambda$  along the current. Using (2.15), we find, instead of (2.14), that

$$\frac{\partial n_1}{\partial t} + \frac{b_1 j(\zeta, \xi, \lambda)}{e b_e} \frac{\partial}{\partial \lambda} \frac{n_1}{n_1 + n_2^{(0)}} = 0. \quad (2.16)$$

Substituting

$$s = \int_{\lambda_0}^{\lambda_1} \frac{j_0}{j(\lambda')} d\lambda',$$

where  $j_0$  is the current density on the boundary, we obtain an equation that is identical with (2.4):

$$\frac{\partial n_1}{\partial t} + V(n_1) \frac{\partial n_1}{\partial s} = 0,$$

where

$$V = \frac{j_0(\zeta, \xi) b_1 n_2^{(0)}}{e b_e (n_1 + n_2^{(0)})^2}.$$

Thus, the breaking of the profile occurs along the current lines.

For the spherically symmetric case, for example, we have

$$\frac{\partial n_1}{\partial t} + \frac{b_1 n_2^{(0)} I}{e b_e (n_1 + n_2^{(0)})^2} \frac{\partial n_1}{\partial \Omega} = 0,$$

where  $\Omega$  is the volume and  $I$  the total current. conservation of the number of particles leads to the area rule in terms of the coordinates  $n_1, \Omega$ .

### D. Three-component plasma with constant mobilities

Let us now consider the evolution of a plasma profile consisting of electrons and several types of ion with constant mobilities  $b_e$  and  $b_1, \dots, b_{k-1}$ . Substituting  $I_\alpha = R_\alpha = 0$ , neglecting diffusion, and using the quasineutrality condition

$$n_e = \sum_{\alpha=1}^{k-1} n_\alpha, \text{ we find from (1.1)–(1.2) that}$$

$$\frac{\partial n_\alpha}{\partial t} + b_\alpha E_0 \sum_{\beta=1}^{k-1} n_\beta^{(0)} (b_\beta + b_e) \frac{\partial}{\partial x} \frac{n_\alpha}{\sum_{\beta=1}^{k-1} (b_\beta + b_e) n_\beta} = 0, \quad (2.17)$$

$$\alpha = 1, \dots, k-1,$$

$$\sum_{\alpha=1}^{k-1} n_\alpha \frac{b_\alpha + b_e}{b_\alpha b_e} = \psi(x). \quad (2.18)$$

The function  $\psi(x)$  is determined by the initial profile and is independent of time. According to (2.17)–(2.18), an arbitrary initial perturbation should split into  $k-2$  propagating signals and one nonpropagating signal corresponding to the perturbation  $\psi(x)$ . Substituting the dimensionless densities

$$\tilde{n}_\alpha = \frac{n_\alpha (b_\alpha + b_e)}{\psi(x) b_\alpha b_e} \quad (2.19)$$

and the coordinate

$$s = \int_0^x \frac{b_e^2 \psi(x') dx'}{\sum_{\alpha=1}^{k-1} n_\alpha^{(0)} (b_\alpha + b_e)}, \quad (2.20)$$

we obtain, instead of (2.17) and (2.18),

$$\frac{\partial \tilde{n}_\alpha}{\partial t} + b_\alpha E_0 \frac{\partial}{\partial s} \frac{\tilde{n}_\alpha}{\sum_{\sigma=1}^{k-1} \tilde{n}_\sigma q_\sigma} = 0, \quad \alpha = 1, \dots, k-1, \quad (2.21)$$

$$\sum_{\alpha=1}^{k-1} \tilde{n}_\alpha = 1, \quad q_\alpha = \frac{b_\alpha}{b_e}. \quad (2.22)$$

When  $k=3$ , the system (2.21)–(2.22) reduces to an equation analogous to (2.4):

$$\frac{\partial \tilde{n}_1}{\partial t} + \tilde{V}(\tilde{n}_1) \frac{\partial \tilde{n}_1}{\partial s} = \frac{\partial \tilde{n}_1}{\partial t} + \frac{b_1 E_0 q_2 \partial \tilde{n}_1 / \partial s}{[n_1(q_1 - q_2) + q_1]} = 0. \quad (2.23)$$

Consider the evolution of a plasma perturbation. If the initial profiles  $n_{10}(x)$  and  $n_{20}(x)$  are similar:

$$\frac{n_{10}(x)}{n_{20}(x)} = \frac{n_1^{(0)}}{n_2^{(0)}}, \quad (2.24)$$

then it is readily seen from (2.18) and (2.19) that the  $\tilde{n}_{\alpha 0}$  do not depend on  $x$  and are equal to their equilibrium values  $n_{\alpha}^{(0)}$ . Consequently, in this case, the perturbation will not evolve in the drift approximation. The inclusion of diffusion leads to a slow spreading of the initial profile.

On the other hand, when  $\psi(x) = \psi^{(0)}$ ,

$$\frac{n_1(x, t) - n_1^{(0)}}{n_2(x, t) - n_2^{(0)}} = \frac{n_{10}(x) - n_1^{(0)}}{n_{20}(x) - n_2^{(0)}} = -\frac{b_1}{b_2} \frac{b_2 + b_e}{b_1 + b_e}; \quad (2.25)$$

$\tilde{n}_{\alpha} \sim n_{\alpha}$ , so that, according to (2.21), this perturbation will be completely transported by the field out of the initial localization region  $L$ , and a profile with a diffusion shock will form. An arbitrary initial profile of scale  $L$  will decay in the course of time into moving and stationary parts. For  $B_e \gg b_1, b_2$ ,

$$n_{\alpha}(x, t) = \bar{n}_{\alpha}(x) + \tilde{n}_{\alpha}(x, t) + n_{\alpha}^{(0)}, \quad (2.26)$$

where the stationary profile is

$$\bar{n}_{\alpha}(x) = b_{\alpha} \psi(x) \tilde{n}_{\alpha}^{(0)}, \quad (2.27)$$

and the moving profile is

$$\tilde{n}_{\alpha}(x, t) = b_{\alpha} \psi(x) [\tilde{n}_{\alpha}(x, t) - \tilde{n}_{\alpha}^{(0)}] + n_{\alpha}^{(0)}; \quad (2.28)$$

where  $\tilde{n}_{\alpha}(x, t)$  satisfies (2.23) and propagates with velocity  $\tilde{V}(\tilde{n}_{\alpha})$ . It is clear from (2.23) that, for  $b_1 > b_2$ , the backside of the profile  $\tilde{n}_{\alpha}(x, t)$  will break, whereas, for  $b_2 > b_1$ , this will occur on the frontside.

We now consider the case where  $n_{20}(x) = n_2^{(0)}$  and  $n_{10}(x) > n_1^{(0)}$ . From (2.18) and (2.27), we have

$$\frac{\bar{n}_2(x) - n_2^{(0)}}{n_{10}(x) - n_1^{(0)}} = \left( \frac{n_1^{(0)}}{n_2^{(0)}} + \frac{b_1}{b_2} \right)^{-1}. \quad (2.29)$$

Hence, it is clear that, when

$$\frac{n_1^{(0)}}{n_2^{(0)}} + \frac{b_1}{b_2} \ll 1 \quad (2.30)$$

the perturbation of ions of the second kind, which appeared in the region  $L$  during the evolution process, will substantially exceed the initial perturbation of ions of the first kind.

For  $\bar{n}_{\alpha}(x, t)$  we have

$$\bar{n}_1(x, t) = n_1^{(0)} \left( 1 + \frac{b_1 n_2^{(0)}}{b_2 n_1^{(0)}} \right) [\tilde{n}_1(x, t) - \tilde{n}_1^{(0)}] + n_1^{(0)} > n_1^{(0)}, \quad (2.31)$$

$$\bar{n}_2(x, t) = n_2^{(0)} \left( 1 + \frac{b_2 n_1^{(0)}}{b_1 n_2^{(0)}} \right) [(1 - \tilde{n}_1(x, t)) - \tilde{n}_2^{(0)}] + n_2^{(0)} < n_2^{(0)}. \quad (2.32)$$

If only ions of kind 2 are present at infinity, we find that, outside the region of initial perturbation,

$$\bar{n}_1 = 0, \quad \bar{n}_2 = n_2^{(0)} \left( 1 - \frac{\tilde{n}_1 b_2}{n_2^{(0)} b_1} \right) > 0. \quad (2.33)$$

Hence,  $\bar{n}_1$  is less than  $b_1 n_2^{(0)} / b_2$ . Thus, when the initial pertur-

bation is strong, and the maximum value of  $n_{10}$  exceeds  $b_1 n_2^{(0)} / b_2$ , the  $n_1$  profile remains practically unaltered for a long time  $t \lesssim t_1 = n_{10} L / b_1 n_2^{(0)} E_0$ . On the other hand, a plasma sheath may flow out in the direction in which there are practically no ions of kind 2 and  $n_1 \sim n_2^{(0)} b_1 / b_2$ . For  $t > t_1$ , an ambipolar peak containing only ions of kind 2 remains in the region of the initial perturbation.

For plasmas with three kinds of positive ions, we find from (2.18)–(2.22) that, for  $b_e \gg b_{1,2,3}$ , and if we eliminate  $\tilde{n}_2$ ,

$$\begin{aligned} \frac{\partial \tilde{n}_1}{\partial t} + \frac{\partial}{\partial s} \frac{\tilde{n}_1 b_1 E_0}{(q_1 - q_2) \tilde{n}_1 + (q_3 - q_2) \tilde{n}_3 + q_3} &= 0, \\ \frac{\partial \tilde{n}_3}{\partial t} + \frac{\partial}{\partial s} \frac{\tilde{n}_3 b_3 E_0}{(q_1 - q_2) \tilde{n}_1 + (q_3 - q_2) \tilde{n}_3 + q_2} &= 0. \end{aligned} \quad (2.34)$$

This set of equations describes the propagation of two types of signal. Their velocities are different, so that they will, in general, separate after a time  $\sim L / b E_0$ , and can be considered separately. When the third kind of ion is present as a small addition, the first mode is practically the same as (2.23). For the second mode, on the other hand, the nonlinearity is small, and the signal propagation velocity is close to  $V_0 = b_3 E_0$ . A small perturbation  $\tilde{n}_1$  can be obtained from the first equation by expanding the second term into a series and assuming that the propagation velocity is  $V_0$ .

### E. Formation of shocks in gas-discharge plasma

Situations that can be described by separating the profile into drift and steep segments are also possible in real gas-discharge plasmas, but are complicated by the fact that ionization and recombination processes play a very important role, as do processes in regions near the electrodes. Their mechanisms are quite complicated and are usually not well known.

As the first example, consider the evolution of inhomogeneity in a *dc* discharge containing a readily ionizable additive. Assuming that the additive is fully ionized, we find that its density  $n_1$  in the drift approximation is given by

$$\frac{\partial n_1}{\partial t} + b_1 \frac{\partial}{\partial x} n_1 E = 0. \quad (2.35)$$

For the main-gas ions and electrons, we have

$$\frac{\partial n_2}{\partial t} + b_2 \frac{\partial}{\partial x} n_2 E = Z(E) (n_1 + n_2) - \frac{n_2}{\tau}, \quad (2.36)$$

$$j = e (n_1 + n_2) b_e (E)^{1/2} E; \quad (2.37)$$

where  $\tau$  is the recombination lifetime, and the ionization probability  $Z$  and electron mobility  $b_e$  are, in general, functions of the electron temperature  $T_e$ . If the scales exceed the energy relaxation length ( $\sim T_e / eE$ ), the relationship between  $T_e$  and  $E$  is determined by the local balance of Joule heat release and heat transfer.<sup>34</sup>

For  $L \gg b_2 E \tau, l_T$  the density of ions of the main gas can be found by equating to zero the right-hand side of (2.36). Substituting for  $E$  from (2.37) in (2.35), we obtain a nonlinear equation for the additive ion density. The rate of ionization  $Z(E)$  is rapidly varying (usually exponential function of the field:  $Z = \tau^{-1} \exp[-\alpha(n_1 + n_2)/n_2^{(0)}]$ , where  $\alpha \gg 1$  and  $n_2^{(0)}$ ,

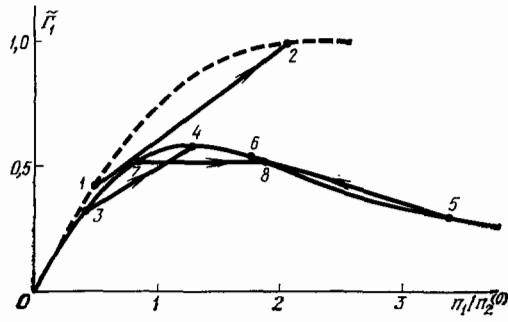


FIG. 2. Flux of ions of fully ionized additive in the drift approximation in units of  $b_1 E_0 n_2^{(0)}$  ( $\alpha = 4$ ).

$E_0$  are, respectively, the ion density and the field in the discharge without the additive. When  $n_1 \lesssim n_2^{(0)}$ , we have  $b_e = \text{const}$  (this approximation is valid for  $b_e$ , for example, when the main gas is helium or hydrogen), and the additive ion flux is

$$\Gamma_1(n_1) = \frac{\alpha b_1 E_0 n_1}{\alpha - \ln [1 - (n_1/n_2^{(0)})]} \quad (2.38)$$

On the other hand, when  $n_1$  is large, the flux  $\Gamma_1 = b_1 j / (e b_e)$  is constant. The function  $\Gamma_1(n_1)$  is shown in Fig. 2 by the broken line. This is accompanied by the breaking of the backside of the additive density profile, and we have the shock  $1 \rightarrow 2$ , in which there is a change in  $n_1, n_2, E, T_e$ . If, on the other hand,  $b_e$  depends on the field, the situation is determined by the form of this dependence. The graph of  $\Gamma_1(n_1)$  for  $b_e \sim E^{-1/2}$  is shown by the solid curve in Fig. 2. Shocks moving along the field ( $3 \rightarrow 4$ ), against the field ( $5 \rightarrow 6$ ), and fixed shocks ( $7 \rightarrow 8$ ) are then possible.

Let us now consider the one-dimensional discharge in a gas flow.<sup>35</sup> We shall consider that  $b_e$  decreases with increasing field. The ambipolar drift velocity is then nonzero, even in simple plasma, and is given by<sup>12,35</sup>

$$V(n) = \frac{d\Gamma}{dn} = \frac{b_1 j}{e} \frac{d}{dn} b_e^{-1}(E) + U, \quad (2.39)$$

where  $U$  is the flow velocity. The relation between  $E$  and  $n$  is set by the conservation of current:  $eEnb_e(E) = j$ . The first term in (2.39) is negative and is directed away from the cathode. The graph of the flux  $\Gamma(n)$  for different signs of  $U$  is shown in Fig. 3. When  $U < 0$  (curve *a*), only shocks of the form  $1 \rightarrow 2$ , moving toward the anode, can occur. When  $U > 0$  (curve *b*), both moving and stationary shocks are possible, depending on the initial and boundary conditions.

In the stationary case, the plasma density is given by

$$V(n) \frac{dn}{dx} = Z_1(E)n - \beta n^2, \quad (2.40)$$

where  $\beta$  is the recombination coefficient and  $L$  is the length of the discharge gap. When  $U < 0$ , the resultant plasma drift velocity (2.39) points toward the anode. If we apply the boundary condition  $n(L) = \infty$  to the cathode,<sup>36</sup> we find that, with the exclusion of narrow regions near the electrodes, the density profile becomes

$$L - x = \int_n^\infty \frac{|V(n)| dn}{Z(n)n - \beta n^2}. \quad (2.41)$$

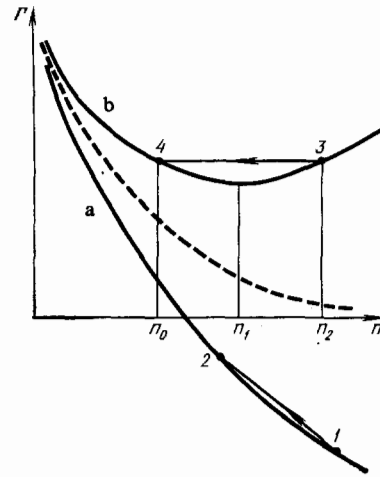


FIG. 3. Drift flux of plasma in a discharge with a flowing gas: a—flow from cathode to anode ( $U < 0$ ); b—flow toward the cathode. Broken curve— $U = 0$ . Equilibrium density  $n_0 = Z(n_0)/\beta$ .

For sufficiently large  $L$ , it describes a continuous fall in the density between the cathode and the equilibrium value  $n_0$ , characteristic for the positive column. The profiles calculated in this way are in good agreement with experiment.<sup>36</sup> If, on the other hand,  $U > 0$ , then, for  $n_0 < n_1$  [ $n_1$  corresponds to the maximum of  $\Gamma(n)$ ], the boundary condition  $n(0) = \infty$  is satisfied by the solution consisting of a smooth segment with a high density at the anode:

$$x = \int_{n_2}^\infty \frac{V(n) dn}{\beta n^2 - Z(n)n},$$

where  $\Gamma(n_2) = \Gamma(n_0)$ , and the shock  $3 \rightarrow 4$ . When, on the other hand,  $n_0 > n_1$ , the solution with the shock satisfies the condition  $n(L) = 0$ . Unfortunately, very little work has been done on boundary conditions in gas-discharge plasmas. In particular, it is not clear which electrode characteristics correspond to particular boundary conditions for our truncated equations. The formation of a sharply inhomogeneous field profile near the anode was observed in Ref. 35. The complicating factor was that filamentation ensued that the discharge at the anode was laterally inhomogeneous. The density in the filaments was much higher than in the main column, but there was a simultaneous increase in the electric field as well. It would appear that, having ensured sufficiently intensive external ionization near the anode [ $n(0) = \infty$ ], it is possible to produce the above laterally inhomogeneous regime with a shock.

### 3. EVOLUTION OF A DISCONTINUITY IN INITIAL CONDITIONS

In general, an initial discontinuity produced in multi-component plasma will disintegrate.<sup>17</sup> For example, in a plasma containing two kinds of positive ions with constant mobilities, an arbitrary discontinuity at  $x = 0, t = 0$  in the densities  $n_1$  and  $n_2$  corresponds to the discontinuity in  $\tilde{n}_1$  and  $\psi$  given by (2.18) and (2.21). According to (2.23), a discontinuity in  $\tilde{n}_1$  that satisfies the evolution condition will propagate with velocity  $\tilde{V}(\tilde{n}_1)$ , but will decay otherwise. When diffusion is taken into account, the equation for  $\psi$  has the following form according to (1.1):

$$\frac{\partial \psi}{\partial t} = D_2 \left( 1 + \frac{T_e}{T_i} \right) \frac{\partial^2}{\partial x^2} \psi \left( 1 + \tilde{n}_1 \frac{D_1 - D_2}{D_2} \right), \quad (3.1)$$

where  $T_{e,i}$  is the electron and ion temperature, respectively. The quantity  $\tilde{n}_1 < 1$  varies smoothly near  $x = 0$  for  $t \neq 0$ , according to (2.23). Hence, the quantity  $1 + \tilde{n}_1(D_1 - D_2)/D_2$  can be taken outside the derivative, and Equation (3.1) then reduces to the diffusion equation with coefficients that are smooth functions of time.

The evolution of discontinuities in initial conditions was observed in Ref. 20 in solutions of binary electrolytes. If the ion mobilities in a fully dissociated solution are functions of density, we have<sup>16,17</sup>

$$\frac{e}{j} \frac{\partial n}{\partial t} + \frac{\partial}{\partial x} \left( \frac{b_1}{b_2 + b_1} \right) = \frac{e}{j} \frac{\partial n}{\partial t} + \frac{\partial R}{\partial n} \frac{\partial n}{\partial x} = 0, \quad n_1 = n_2 = n. \quad (3.2)$$

The ratio  $b_1/(b_2 + b_1) = R(n)$  is called the cation transference number. The evolution of the sharp boundary between two solutions of different density was investigated experimentally. When  $R$  is independent of density, the boundary is fixed and diffuses only as a result of ambipolar diffusion. Its width increases as  $\sqrt{t}$ . If the function  $R(n)$  is nearly linear, the motion of the boundary is found to change when the current is reversed, but its spreading is determined by diffusion, as before. If, on the other hand,  $\partial^2 R / \partial n^2 \neq 0$ , the boundary satisfying the evolution condition  $n^+ > n^-$  for  $\partial^2 R / \partial n^2 < 0$  will propagate with velocity

$$W = \frac{j}{e} \frac{R(n^+) - R(n^-)}{n^+ - n^-}, \quad (3.3)$$

and will not spread by diffusion. When the current is reversed, the boundary should rapidly spread, approximately in proportion to  $t$ . Figure 4 shows the measured refractive index gradient  $dk/dx$  (approximately proportional to the density of the solution) for different directions of the current relative to the density gradient. It is clear that the evolution is in good agreement with the three cases examined above. For KCl, the transference numbers are practically independent of  $n$ , whereas, for CaCl, the function  $R(n)$  is practically linear [the ratio  $R'(n^+ - n^-)/(2R')$  characterizing the non-linearity of  $R(n)$  is equal to about 0.1]. For CdI, this quantity is much greater, i.e., of the order of 0.4.

#### 4. WEAKLY-IONIZED PLASMA IN A MAGNETIC FIELD

##### A. One-dimensional case

In a magnetic field, the situations in which diffusion shocks appear become even more varied. Consider, for example, a one-dimensional plasma inhomogeneity which is infinite in the direction of  $\mathbf{B}$  and  $\mathbf{E}_0 \times \mathbf{B}$  and contains ions of two kinds.<sup>29</sup> We shall suppose that  $\beta = 8\pi n t / B^2 \ll 1$ , so that the perturbation of the magnetic field is unimportant. The ion density  $n_1$  vanishes as  $y \rightarrow \infty$  (the  $y$  axis lies along the electric field) and  $n_2$  forms a uniform background at the initial time:  $n_2(y, 0) = n_2^{(0)}$ . In a strong enough magnetic field, the mobility and diffusion of electrons across the magnetic field are negligible in comparison with the corresponding ion parameters. Hence, in the absence of generation and recombination, the total plasma density is

$$n_1 + n_2 = n(y, t = 0). \quad (4.1)$$

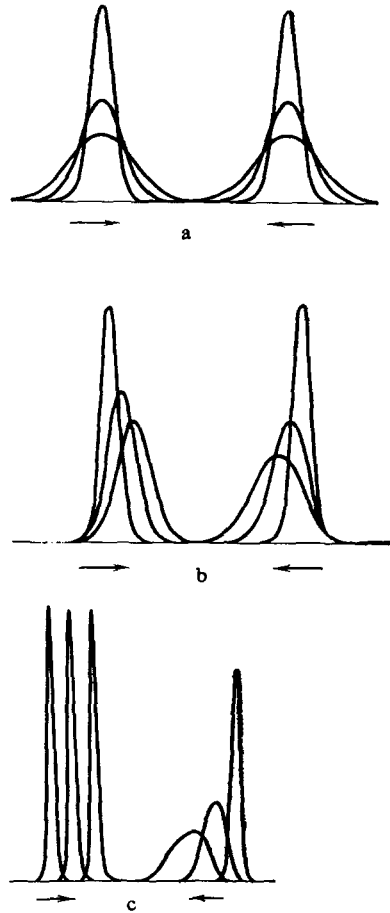


FIG. 4. Evolution of the  $dk/dx$  profile when the current flows through the initially sharp boundary between the two solutions. The right and left families of curves refer to opposite current directions. The successive profiles were recorded at intervals of 2 hours. The solution densities  $n^+$  and  $n^-$  are: a—0.2N:0.5N, KCl; b—0.1N:0.2N, CaCl<sub>2</sub>; c—0.1N:0.2N, CdI.

Neglecting diffusion, we find from the continuity equations that

$$\frac{E}{E_0} = \frac{b_{2\perp} n_2^{(0)}}{b_{1\perp} n_1 + b_{2\perp} n_2}, \quad (4.2)$$

$$\frac{\partial n_1}{\partial t} + b_{1\perp} b_{2\perp} E_0 n_2^{(0)} \frac{\partial}{\partial y} \frac{n_1}{b_{1\perp} n_1 + b_{2\perp} n_2} = 0. \quad (4.3)$$

The solution of (4.3) is

$$g(s, t) = \left( 1 - \frac{b_{1\perp}}{b_{2\perp}} \right) \frac{n_1}{n} = g_0 \left[ s - \frac{b_{1\perp} E_0 t}{(1 - g_0)^2} \right], \quad (4.4)$$

where

$$s = \int_0^y dy \frac{n(y)}{n_2^{(0)}}.$$

In terms of the coordinates  $s, t$ , the rate of displacement of points on the profile,  $\tilde{V}(g) = b_{1\perp} E_0 / (1 - g)^2$ , increases with increasing  $g$ , which for  $b_{1\perp} < b_{2\perp}$  corresponds to the breaking of the frontside.

This problem is of interest in connection with the evolution of plasma clouds in the ionosphere. When this type of cloud has a sufficiently large transverse dimension, the ionospheric plasma can be described by the so-called two-layer

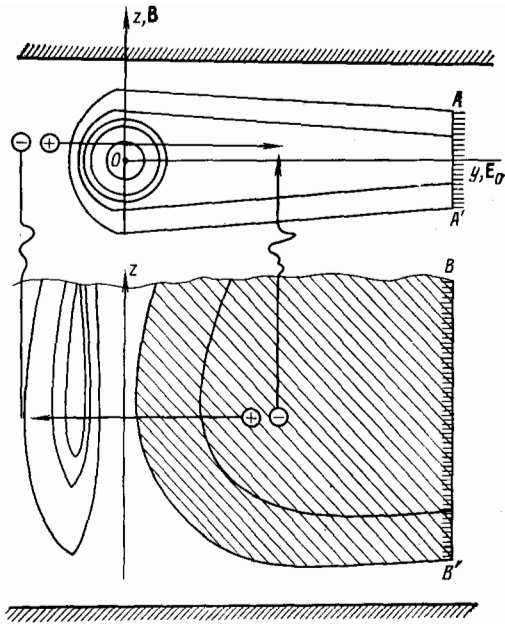


FIG. 5. Closure of currents in the ionosphere. The initial inhomogeneity was produced at the origin. The upper part shows lines of constant density of injected ions and the lower part of the background plasma. The depletion region is shaded. Diffusion shocks are indicated by  $A-A'$ ,  $B-B'$ .

model.<sup>37</sup> The magnetic lines of force are then regarded as equipotentials, and the ionosphere under the cloud is approximately described by a layer of plasma bounded in the direction of the magnetic field by dielectric walls, with mean mobility  $\hat{b}_2$  and density  $N_2$  integrated along the height (along  $B$ ). (For a discussion of this model, see Refs. 29 and 30.) Injected ions are characterized by the integrated density

$$N_1 = \int n_1 dz$$

and mobility  $\hat{b}_1$  at the height of escape. Many features of the evolution of real plasma clouds can be understood by analyzing the one-dimensional problem, namely, a plasma filament that is infinite in the Hall direction.

Since electrons can effectively flow only along  $B$ , and redistribute themselves between the inhomogeneity and the background ionospheric plasma, we have  $N_1 + N_2 = N(y)$

by analogy with (4.1). The injected-ion current is compensated by the background current flowing in the opposite direction, as shown schematically in Fig. 5. So long as the displacement of ions in the vertical direction is unimportant, the equations describing the evolution of the quantities  $N_{1,2}$  are the same as (4.1)–(4.3) except that  $n_{1,2}$  is replaced with  $n_{1,2}$ .

The solution of (5.3) for an initial perturbation of the form

$$N_1(y, t=0) = AN_2^{(0)} \exp\left(-\frac{y^2}{a^2}\right), \quad A > 1, \quad (4.5)$$

was analyzed in Ref. 29.

Since the mobility of ions across the magnetic field in the ionosphere decreases rapidly with height, we have  $b_{2\perp} \gg b_{1\perp}$ . Provided  $A$  is not too large, and satisfies the condition

$$1 < A < \frac{b_{2\perp}}{b_{1\perp}}, \quad (4.6)$$

the solution given by (4.4) is as illustrated in Figs. 6 and 7. Analysis of (4.4) readily shows<sup>29</sup> that the rate at which the injected particles  $N_1$  flow out is variable. Initially, for  $t \lesssim t_1 = a(b_{1\perp} E_0 A)^{-1}$  (this stage is illustrated in Fig. 6), the field is only slightly perturbed and the original  $N_1$  profile moves with velocity  $\sim b_{1\perp} E_0$ . It is only on the frontside of the profile that the formation of a depletion region in the background plasma produces an increase in the field up to  $\sim E_0 A$ , so that the rate at which the ions  $N_1$  flow out becomes very high ( $\sim b_{1\perp} E_0 A$ ). Background ions ejected from the depletion region fill the original profile and reduce the electric field in this region. A substantial reduction occurs in the time in which  $n_1$  at the center of the profile becomes  $\sim N_2^{(0)}$ , i.e., in the time  $\sim t_1$ . This is accompanied by the formation of a shock on the frontside. For  $t \gg t_1$ , the rate at which the injected ions flow out falls to  $b_{1\perp} E_0$ , so that a substantial fraction of them flows out of the original profile for a long time  $\sim Aa/b_{1\perp}|E_0$  (see Fig. 7). When  $A > b_{2\perp}/b_{1\perp}$ , it follows from (4.2)–(4.4) that the electric field inside the inhomogeneity is low right from the outset:  $E \sim E_0/A$ , and the rate of outflow of injected ions is of the order of  $b_1 E_0$ .

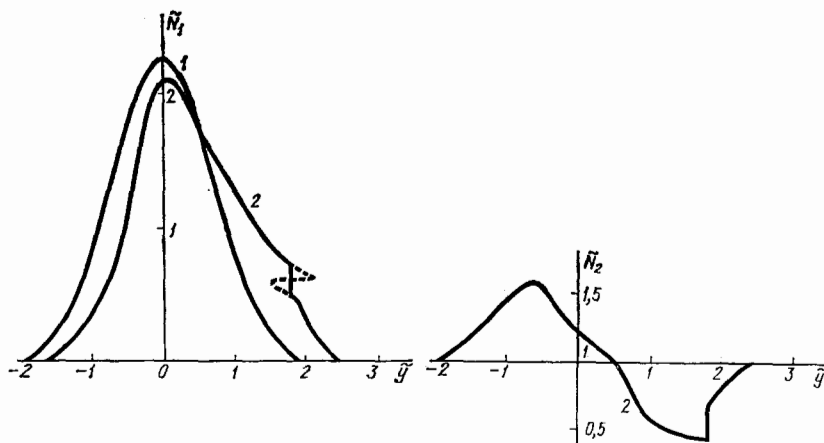


FIG. 6. Graphs of  $\tilde{N}_{1,2} = N_{1,2}/N_2^{(0)}$  for  $b_{11} = 0.2b_{21}$ ,  $A = 4/\sqrt{\pi}$ . Curve 1—initial profile of  $\tilde{N}_1$ ; curve 2— $t = 0.5a/b_{1\perp} E_0$ ,  $ty = y/a$ .



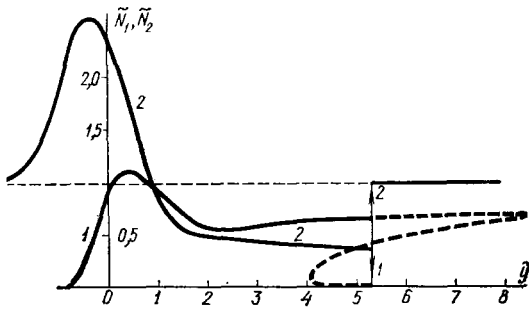


FIG. 7. Graphs of  $\tilde{N}_1$  (1) and  $\tilde{N}_2$  (2) for the same conditions as in Fig. 6 at time  $t = 2a/b_{11} E_0$ .

### B. Shocks, in the Hall direction

The difference between the electric field (in the direction of  $\mathbf{E}_0$ ) on the edge and at the center of the profile has an important effect on the Hall motion of real inhomogeneities. When (4.6) is satisfied, this difference should lead to the stretching of the plasma bunch in the Hall direction, and appreciable deformation should occur in a time  $\sim t_1$ . This phenomenon has been observed in two-dimensional numerical calculations<sup>28</sup> (Fig. 8). As can be seen, there are large density gradients, which correspond to diffusion shocks occurring both in the direction of  $\mathbf{E}_0$  and in the Hall direction.

The analytic expression describing the appearance of the shock in the Hall direction can be readily obtained in the simple example examined in Ref. 30. Suppose that  $b_1 = b_2$ ,  $A \gg 1$ , and that the original inhomogeneity  $N_1$  is elongated in the direction of  $\mathbf{x} \parallel \mathbf{E}_0 \times \mathbf{B}$ . In the two-dimensional case, instead of (4.3) we have

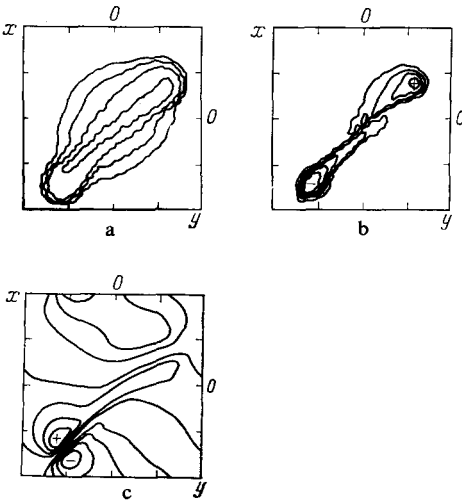


FIG. 8. Lines of constant density of injected (a) and background (b) ions and equipotentials (c) obtained by numerical simulation of the evolution of a barium cloud in the ionosphere, using the two-layer model.<sup>28</sup> The coordinate frame moves along the  $x$  axis with drift velocity  $cE_0/B$ ;  $b_{11}/b_{21} = 1.25 \times 10^{-2}$ , which corresponds to injection at a height of 200 km;  $A = 8$ ; the scale is in units of  $2a = 8$  km; the time after injection is  $aB/cE_0 \approx 0.8t_1$ . The background-plasma depletion region lies in the left bottom corner of Fig. b. The fact that the inhomogeneity is pulled at an angle to the Hall direction is due to the presence of the Hall current in the background plasma ( $b_{21} \sim b_{2H}$ ).

$$\frac{\partial N_\alpha}{\partial t} + b_{\alpha\perp} \nabla_\perp \cdot N_\alpha \mathbf{E} + b_{\alpha H} \left( E_y \frac{\partial N_\alpha}{\partial x} - E_x \frac{\partial N_\alpha}{\partial y} \right) = 0, \quad (4.7)$$

where  $\alpha = 1, 2$  and  $b_{\alpha H}$  are the Hall mobilities. We shall suppose that the ions are magnetized, so that  $b_{eH} = b_{iH} = c/B$ .

For electron density  $N = N_1 + N_2$ , instead of (4.1) we have

$$\frac{\partial N}{\partial t} + b_H \left( E_y \frac{\partial N}{\partial x} - E_x \frac{\partial N}{\partial y} \right) = 0. \quad (4.8)$$

When the inhomogeneity is elongated in the  $x$  direction, the conservation of current

$$\nabla_\perp \cdot (N\mathbf{E}) = 0 \quad (4.9)$$

gives rise to the same field as in the one-dimensional case:  $E_y = E_0 N_2^{(0)}/N$ . Let us now consider the evolution of the profile near  $y = 0$ . If the initial inhomogeneity is symmetric in  $y$ , the resultant density is such that  $\partial N / \partial y|_{y=0} = 0$  at all times. Hence, we can neglect the last term in (4.8):

$$\frac{\partial N}{\partial t} + \frac{b_H E_0 N_2^{(0)}}{N} \frac{\partial N}{\partial x} = 0. \quad (4.10)$$

This equation describes a breaking wave, and the shock occurs on the backside of the inhomogeneity (in the direction of  $\mathbf{E} \times \mathbf{B}$ ) while  $N_1^+ > N_1^-$  on the discontinuity. The steepening of the backside in the Hall direction has frequently been observed in experiments with barium clouds in the ionosphere. A typical example<sup>38,39</sup> is shown in Fig. 9. The numerical solution of (4.8)–(4.9) reported in Refs. 37 and 40 also indicates a steepening of the backside of the inhomogeneity. It was also shown in Refs. 37 and 40 that a gradient drift instability develops in the region of the shock, and this leads to its turbulization. On the other hand, the barium-plasma tail that flows out in the Hall direction is stratified. In other words, and instability is also found to develop in this region. A possible mechanism of stratification, involving the inertial drift of ions in the nonstationary inhomogeneous electric field, was proposed in Ref. 41. Density profiles averaged over the strata, and the rate of outflow of plasma from the cloud, are in good agreement<sup>38,39</sup> with (4.10). In numerical calculations, a shock in the Hall direction was obtained within the framework of the complete three-dimensional set of equations describing the evolution of the inhomogeneity against the background of unbounded homogeneous plasma (Fig. 10).

### C. Effect of ionization and recombination on the evolution of shocks

These phenomena correspond to the spatial scale  $W\tau$ , where  $W$  is the velocity of the shock and  $\tau$  is the characteristic relaxation time. We shall suppose that it is much greater than the thickness of the diffusion shocks, but much smaller than the scale of the initial profile. Then, as in gas dynamics,<sup>14,15</sup> discontinuities can form in drift solutions consisting of a diffusion shock and a relaxation wave.

Suppose that, in the example of subsection A considered above, there is rapid recombination of ions of kind 2 (Ref. 30):

$$\frac{\partial N_2}{\partial t} + b_{2\perp} \frac{\partial}{\partial y} (EN_2) = \frac{N_2^{(0)} - N_2}{\tau}. \quad (4.11)$$

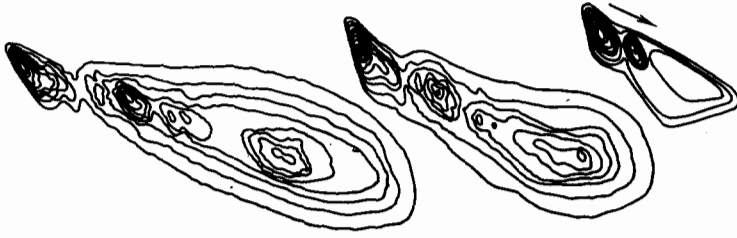


FIG. 9. Cloud of  $Ba^+$  ions in the Spolokh-1 experiment<sup>38,39</sup> at different times. The lines correspond to an equal number of particles along the line of sight. The arrow shows the direction of drift in crossed fields in the reference frame moving with the neutral-particle wind velocity. The Hall shock is produced on the backside of the inhomogeneity.

As  $\tau \rightarrow 0$ , we have from (4.3)

$$\frac{\partial N_1}{\partial t} + \frac{\partial \Gamma_1}{\partial y} = -\frac{\partial N_1}{\partial t} + b_{1\perp} b_{2\perp} E_0 N_2^{(0)} \frac{\partial}{\partial y} \frac{N_1}{b_{1\perp} N_1 + b_{2\perp} N_2^{(0)}} = 0. \quad (4.12)$$

The shock is formed on the backside of the profile for any ratio of  $b_{1\perp}$  and  $b_{2\perp}$ . Its structure can be investigated by transforming to the system  $X = y - Wt$ , which moves with velocity  $W$ . Assuming, for simplicity, that  $b_{1\perp} = b_{2\perp} = b$ , we obtain

$$W \frac{\partial N_1}{\partial X} = N_2^{(0)} b E_0 \frac{\partial}{\partial X} \frac{N_1}{N}, \quad (4.13)$$

$$W \frac{\partial N}{\partial X} = (N - N_1 - N_2^{(0)}) \tau^{-1},$$

$$N_1 \left( W - \frac{b E_0 N_2^{(0)}}{N} \right) = N_1^- \left( W - \frac{b E_0 N_2^{(0)}}{N^-} \right) \equiv K. \quad (4.14)$$

The solution, for which  $N = N_1 + N_2$  becomes  $(N_1^+ + N_2^{(0)})$ ,  $(N_1^- + N_2^{(0)})$  for  $X \rightarrow \pm \infty$ , corresponds to  $K = -W n_1^+ N_1^- / N_2^{(0)}$ . Equation (4.13) then becomes

$$\frac{dN}{dX} = \frac{(N - N^-)(N^+ - N)}{(1 - WN)\tau}, \quad (4.15)$$

i.e., it describes a transition on a scale  $\sim W\tau$ ,  $N^+ > N^-$ .

When the time is large in comparison with the breaking time, we have  $N_1^- \ll N_1^+$  and  $K \rightarrow 0$ ,  $W \rightarrow b E_0 N_2^{(0)} / (N_1^+ + N_2^{(0)})$ . In this case as  $X \rightarrow +\infty$ , the densities  $N$ ,  $N_1$

vary very rapidly, and diffusion becomes important. The  $N_1$ ,  $N_2$  profiles then consist of two portions, the first of which is analogous to the relaxation zone of a shock wave,<sup>14,15</sup> and has the scale  $W\tau$ :

$$N_1 = 0, \quad N_2 = N = N_2^{(0)} + B \exp\left(-\frac{X}{W\tau}\right). \quad (4.16)$$

In this region,  $N_2$  rises from  $N_2^{(0)}$  to  $(N_2^{(0)} + N_1^+)$ . The diffusion shock lies on its right boundary. Since its thickness is small, the density  $N$  is continuous in its interior,  $N_2$  falls to  $N_2^{(0)}$ , and  $N_1$  rises to  $N_1^+$ . Hence,  $B = N_1^+ \exp(-X_c/W\tau)$  in (4.16), where  $X_c$  is the coordinate of the diffusion shock.

## 5. PARTIALLY AND FULLY IONIZED PLASMA

### A. Partially ionized plasma in a magnetic field

Inclusion of electron-ion collisions leads to the formation of shocks even in simple plasma consisting of ions of a single kind.<sup>22</sup> In a magnetic field, the particle fluxes are related to  $\mathbf{E}$  by

$$\Gamma_{e,i} = \mp \hat{b}_{e,i} \mathbf{E}, \quad (5.1)$$

where  $\hat{b}_{e,i}$  are the mobility tensors which depend on density.<sup>42</sup> In the one-dimensional case, current conservation in the direction of the inhomogeneity  $\mathbf{q}$  yields

$$E_{\mathbf{q}} = \frac{n_0}{n} [(\hat{b}_e + \hat{b}_i)^{-1} (\hat{b}_e^{(0)} + \hat{b}_i^{(0)}) \mathbf{E}_0]_{\mathbf{q}}. \quad (5.2)$$

Substituting this into the continuity equation and neglecting diffusion, we obtain the following first-order nonlinear equation<sup>22</sup>:

$$\frac{\partial n}{\partial t} + \frac{\partial}{\partial n} \left[ -n_0 \frac{(b_{e\parallel} \cos^2 \beta + b_{e\perp} \sin^2 \beta) (\hat{b}_i^{(0)} \mathbf{E}_0)_{\mathbf{q}} + (b_{i\parallel} \cos^2 \beta + b_{i\perp} \sin^2 \beta) (\hat{b}_e^{(0)} \mathbf{E}_0)_{\mathbf{q}}}{(b_{e\parallel} + b_{i\parallel}) \cos^2 \beta + (b_{e\perp} + b_{i\perp}) \sin^2 \beta} \right] \times \frac{\partial n}{\partial q} = 0, \quad (5.3)$$

where  $\beta$  is the angle between  $\mathbf{q}$  and  $\mathbf{B}$ . In the absence of a magnetic field, the mobility ratio

$$\frac{b_{e\parallel}}{b_{i\parallel}} = \frac{e}{m_e (v_{ea} + v_{ei})} \left( \frac{e}{m_i v_{ia}} \frac{v_{ea}}{v_{ea} + v_{ei}} \right)^{-1} = \frac{m_i v_{ia}}{m_e v_{ea}} \quad (5.4)$$

is independent of density. Hence, the velocity of the signal is zero:

$$V(n) = E_0 n_0 (b_{e\parallel}^{(0)} + b_{i\parallel}^{(0)}) \frac{\partial}{\partial n} \frac{b_{i\parallel}}{b_{e\parallel} + b_{i\parallel}} = 0$$

and the diffusion shock does not occur despite the fact that the mobilities themselves can be very dependent on density. In a magnetic field, on the other hand, a rapidly varying  $V(n)$

can occur, according to (5.3), when  $v_{ea} \sim v_{ei}$  if the plasma magnetization is  $\omega_{ce} \omega_{ci} / v_{ea} v_{ia} \sim 1$  ( $\omega_{ce,i}$  are the cyclotron frequencies). The corresponding example for  $\mathbf{q} \parallel \mathbf{E}_0 \times \mathbf{B}$  is given in Ref. 22. When the magnetic fields are strong,  $V(n)$  tends to zero whatever the orientation of the inhomogeneity relative to  $\mathbf{E}_0$  and  $\mathbf{B}$ .

### B. Fully ionized plasma in zero magnetic field

In this case, diffusion shocks occur in multicomponent plasmas containing ions with different charges  $z_\alpha$ . Let us consider isothermal fully ionized plasmas containing ions of two kinds, namely, singly-charged ions 1 and ions 2 of

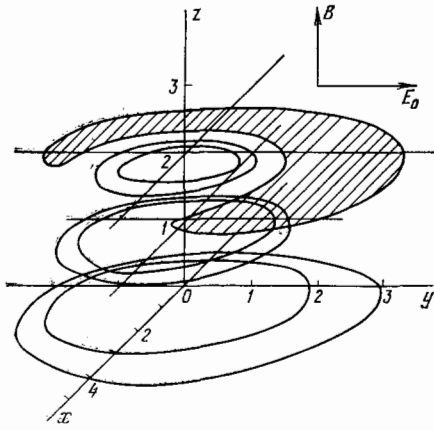


FIG. 10. Three-dimensional evolution of an initially Gaussian profile  $n_1(r,0) = An_2^{(0)} \exp(-r^2/a^2)$  on a background of a homogeneous isothermal weakly ionized plasma in crossed fields, with allowance for drift and diffusion.  $A = 25$ ;  $b_{eH} = b_{1H} = b_H$ ;  $b_{e1} = 0$ ;  $b_{e11} = 1.25b_H$ ;  $b_{i1} = 0.5b_H$ . The time corresponds to the instant  $1.6ea^2/Tb_H = 1.6a/E_0b_H$ ;  $E_{oy} = T/ea$ ; the coordinates are given in units of  $a$ . Level lines in the  $z = 1-3$  sections correspond to total plasma densities of  $1.5n_2^{(0)}$  and  $2n_2^{(0)}$ . The depletion region is shaded at the  $0.9n_2^{(0)}$  level. As can be seen, the profile is highly twisted in the direction of  $E_0 \times B$ .

charge  $eZ$ . The system is quasineutral and isobaric if

$$n_e \equiv n = n_1 + Zn_2, \quad (5.5)$$

$$n + n_1 + n_2 = \frac{p_0}{T}. \quad (5.6)$$

Ignoring inertia and pressure gradients of the components, we find that the equations of motion are

$$eE + \alpha_{e1}n_1(v_e - v_1) + \alpha_{e2}n_2(v_e - v_2) = 0, \quad (5.7)$$

$$eE + \alpha_{e1}n(v_e - v_1) - \alpha_{i2}n_2(v_1 - v_2) = 0; \quad (5.8)$$

where  $\alpha_{e2} \simeq Z^2\alpha_{e1}$ ,  $\alpha_{e1}/\alpha_{i2} \sim \sqrt{m_e/M_i}/Z^2$ . If the plasma is at rest at infinity, then  $v_e \gg v_1, v_2$  and

$$v_e = -\frac{j}{en} = -\frac{eE}{\alpha_{e1}n_1 + \alpha_{e2}n_2}, \quad (5.9)$$

where  $j$  is the current density. Substituting (5.5)–(5.9) into the continuity equations for ions, given by (1.1)–(1.2), we obtain the nonlinear equation describing the breaking wave:

$$\frac{\partial n}{\partial t} + \frac{\partial}{\partial x} \left\{ \frac{(p_0 - 2nT)(Z+1)}{p_0(Z-1)} \left[ \frac{(\alpha_{e2} - Z\alpha_{e1})j}{e\alpha_{i2}n} \frac{Zp_0}{T(Z+1)} - F \right] \right\} = 0, \quad (5.10)$$

where

$$F = \frac{j}{e} \frac{(\alpha_{e2} - Z\alpha_{e1})}{\alpha_{i2}} + \left[ \frac{Zp_0}{T(Z+1)} - n_0 \right] v_1^{(0)} - \left( n_0 - \frac{p_0}{2T} \right) v_2^{(0)}.$$

The expression in the braces in (5.10) can be interpreted as the flux  $\Gamma(n)$ . Since  $d^2\Gamma/dn^2 > 0$ , the evolution condition leads to  $n^+ < n^-$ . In other words, since points on the profile with lower values of  $n$  move against the field  $E_0$  more rapidly, the frontside of the plasma density profile should break. This situation occurs in the region near the wall of a tokamak or in high-current arc discharges in which the temperature and mean free paths are large and the impurity density may be considerable.

### C. Fully ionized plasma in a magnetic field

As in the case of weakly or partially ionized plasmas, a much greater variety of diffusion shocks can occur when a magnetic field is present. Let us consider the example of shocks produced in the Hall direction, which recalls the situation in weakly ionized plasma (cf. Section 4D). Suppose that a plasma bunch of density  $n_1(x, y, z)$  is allowed to enter a fully ionized plasma of density  $n_2(z)$ , which is bounded by dielectric walls parallel to  $B(B \parallel z)$ . The bunch enters along the  $x$  direction. The deceleration of the bunch produces an inertial drift of the ions in the  $y$  direction, which gives rise to the field  $E_y$  that maintains the motion of the plasma in the original direction. The variable field  $E$  generates MHD waves propagating in the background plasma. These waves are damped out in a time of the order of the skin time, and the electric field becomes potential.

The evolution of the electric field occurs in two stages. In the first stage, the field is transported along  $B$  because of the high mobility of electrons. The inertial current in the inhomogeneity is closed during this period by the inertial counter current in the background plasma, and terms  $(v \cdot \nabla)v$  can be neglected in comparison with  $\partial v/\partial t$ . Assuming, for simplicity, that the masses of the background and injected ions are equal, we have

$$\text{div}_{\perp} \int_0^{L_z} \frac{m_i c^2}{B^2} [n_1(x, y, z) + n_2(z)] \frac{\partial E_{\perp}}{\partial t} dz = 0. \quad (5.11)$$

When  $L_z$  is not too large,  $E$  will cease to depend on  $z$  at the end of the fast stage (by analogy with the two-layer model of Section 4A). Integrating (5.11) with respect to time, we therefore obtain, at the end of the fast stage,

$$\nabla_{\perp} N (E - E_0) = 0, \quad (5.12)$$

where  $N = N_1 + N_2$ ,

$$N_{1,2} = \int_0^{L_z} n_{1,2} dz$$

are the integrated particle densities in the inhomogeneity and the background plasma, respectively,  $E_0 = Bv_0/c$ , and  $v_0$  is the initial velocity of the bunch. Equation (5.12) is the initial condition for the slow stage and defines  $E$  as a function of  $N$ . It is identical with (4.9) to within  $E_0$  for a cloud of weakly ionized plasma in the two-layer model. The electric field does not depend on  $z$  during the slow stage. Since  $B$  is not perturbed at the boundaries  $z = 0, L_z$ , the total current in the  $x, y$  plane is zero:

$$\left( \frac{\partial}{\partial t} + v \cdot \nabla \right) v = 0, \quad (5.13)$$

where

$$v = cE \times B/B^2. \quad (5.14)$$

The continuity equation for the bunch ions is

$$\frac{\partial N_1}{\partial t} + (v \cdot \nabla) N_1 = 0. \quad (5.15)$$

These equations describe the isothermal motion of an incompressible fluid. The flows described by (5.13) and (5.14) constitute a special case of plane MHD flows<sup>43,44</sup> corresponding to a constant magnetic field. The set of equations (5.13)–

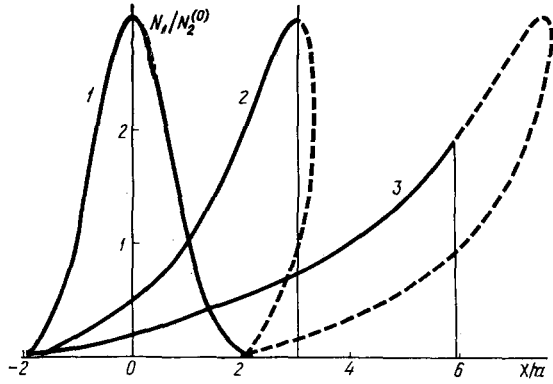


FIG. 11. Evolution of a moving plasma bunch with an initial Gaussian profile  $AN_2^{(0)} \exp(x^2/a^2)$ .  $A = 3$ ; 1—initial profile; 2— $t = 4a/v_0$ ; 3— $t = 10a/v_0$ .

(5.15) have the solution

$$N_1(r, t) = N_{10}(s - |V(N_{10})|t), \quad (5.16)$$

where  $s$  is the path traversed by the particle of the fluid (plasma) in a time  $t$ , and the velocity  $V(N_1) \equiv v$  is determined by (5.12) and (5.14). When the inhomogeneity is elongated along the  $x$  axis, we have at the end of the fast stage

$$E_y = \frac{N_{10}}{N_0} E_0, \quad (5.17)$$

so that, for small  $y$ , the solution (5.16) describes breaking of the wave with a shock on the frontside as shown in Fig. 11.

In the presence of external fields, or a magnetic field inhomogeneity, instead of (5.13) we have

$$\frac{\partial \mathbf{v}}{\partial t} + (\mathbf{v} \cdot \nabla) \mathbf{v} = \mathbf{g} \frac{N_1}{N}, \quad (5.18)$$

where  $\mathbf{g}$  is the corresponding acceleration. For an inhomogeneity elongated along the  $x$  axis, the displacement of points on the profile  $N_1$  for small  $y$  with  $\mathbf{g} = \text{const}$  during the slow state is

$$x = v_0 t + \frac{g t^2 N_{10}}{2N_0} \quad (5.19)$$

The appearance of steep profiles in this situation was observed in Ref. 45, where the acceleration was produced by toroidal drift of the plasma. When the particle density was small in comparison with the background density, the profile was practically immobile. The center of the dense bunch was moving in accordance with (5.18), the acceleration being independent of density (Fig. 12).

## 6. DIFFUSION SHOCKS IN SEMICONDUCTION PLASMA

### A. Evolution of the profile as carriers heat up in a semiconductor with fully ionized donors

In strong fields, the mobility of carriers depends on the field  $E$ . In the case of simple plasma ( $p = n$ , where  $p, n$ , are the densities of holes and electrons, respectively), the rate of ambipolar drift is then nonzero.<sup>12</sup> We shall confine our attention to a model of n-type semiconductor with  $b_n \gg b_p$ , when only the heating of electrons is important and<sup>25</sup>

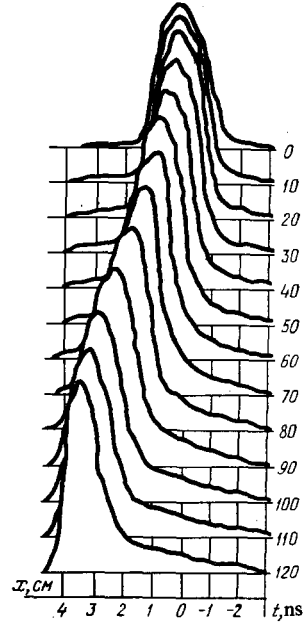


FIG. 12. Motion of a dense plasma bunch injected with zero initial velocity into a bent toroidal  $Q$ -machine in the presence of background plasma.<sup>45</sup> The displacement of the bunch center corresponds to (5.18) with  $\mathbf{g} \approx cT/eBR$ .

$$b_n(E) = \begin{cases} b_{n0} & \text{for } E < E_h, \\ b_{n0} \sqrt{\frac{E_h}{E}} & \text{for } E > E_h. \end{cases} \quad (6.1)$$

The current of holes in the drift approximation is given by

$$\Gamma_p(p) = \begin{cases} \frac{\Gamma_0 p}{p + N_D} & \text{for } p < p_h, \\ \Gamma_0 \frac{j}{j_h} \frac{p N_D}{(p + N_D)^2} & \text{for } p > p_h; \end{cases} \quad (6.2)$$

where  $\Gamma_0 = j b_p / e b_{n0}$ ,  $j_h = e E_h b_{n0} N_D$ ,  $p_h = N_D (j / j_h - 1)$ ,  $N_D$  is the density of donors, and the density region  $p < p_h$ ,  $j > j_h$  corresponds to hot electrons.

When  $j > 2j_h$ , the graph of  $\Gamma_p(p)$  has a descending segment on which  $V(p) < 0$  (Fig. 13). In this situation, we can have stationary shocks and shocks moving to the left or right. In the shock "under the hump," the diffusion current is negative, so that the density increases in the direction of

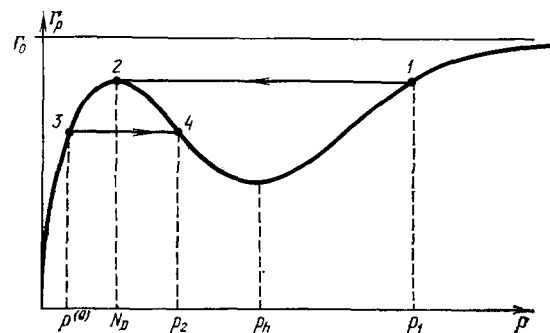


FIG. 13. Drift flux of holes in an n-type semiconductor with appreciable heating of electrons.

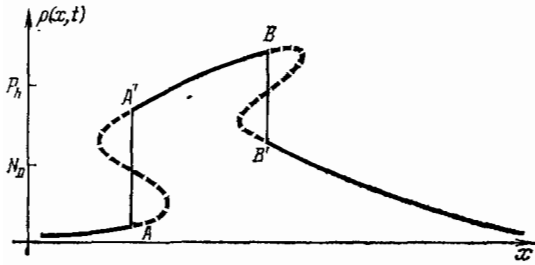


FIG. 14. Evolution of a Gaussian profile for  $p^{(0)} = 0$ ,  $AN_D > p_h$ .

the field  $E$ . Contrariwise, the shock "above the well" is possible only if the density decreases.

Suppose that the equilibrium concentration corresponds to  $p^{(0)} < N_D$  and that the maximum initial density in the Gaussian profile  $p$  (see Fig. 1a) exceeds  $p_h$  (Ref. 31). In the course of time, sections of the profile with  $N_D < p < p_h$  shift to the left (against the field), the remaining sections shift to the right. The points where  $p = N_D p_h$  remain where they were. As a result a region of increased plasma density is formed bounded by two diffusion shocks (Fig. 14). In the process of evolution the shocks coalesce ( $B$  coincides with  $A'$ ), and the single  $A \rightarrow B'$  shock is produced. Subsequently, the wave decreasing in amplitude moves to the right, and asymptotically approaches a triangular wave.

### B. Stationary profiles with shocks

Stationary shocks are also possible in this situation. They were observed in Refs. 23 and 24 when hot carriers were injected and accumulated in n-InSb. Injection into a semi-infinite specimen is described by the drift equation

$$\frac{d}{dx} \Gamma_p(p) = -\frac{p-p^{(0)}}{\tau} = -R(p, p^{(0)}) \quad (6.4)$$

with the boundary condition  $p(0) = \infty$  (Ref. 9), where  $\tau$  is the lifetime of the excess carriers. When  $E < E_h$ , this describes the smooth reduction in density down to the equilibrium value  $p^{(0)}$ , with a scale of the order of the drift length  $l_E = b_p E \tau$ . However, the situation changes as the current increases. The drift solution for  $j > 2j_h$ ,  $p^{(0)} < p_h$  becomes impossible. Actually, the hole current should decrease as a result of recombination, whereas according to (6.3) the drift current should increase in the interval  $(p_h, N_D)$ . This results in a stationary diffusion shock.<sup>25</sup> When  $p^{(0)} < N_D$ , the concentrations on its boundaries are  $N_D, p_1$ , where  $\Gamma_p(p_1) = \Gamma_p(N_D)$  (1  $\rightarrow$  2 in Fig. 13<sup>5</sup>). The drift solution is valid between  $p = \infty$  and  $p = p_1$ , and between  $p = N_D$  and  $p = p^{(0)}$ . When  $j > 4j_h$ , we have  $\Gamma_p(N_D) > \Gamma_0$ , so that the shock reaches the anode and the injection level is low throughout the specimen ( $p < N_D$ ). When  $p^{(0)} > N_D$ , the density in the shock decreases from  $p_1$  to  $p^{(0)}$ , where  $\Gamma(p^{(0)}) = \Gamma(p_1)$ . Hence, injection with a large scale  $l_E$  is generally impossible for  $\Gamma(p^{(0)}) > \Gamma_0$ .

The collecting contact (cathode) in the n-type specimen corresponds to the boundary condition  $\Gamma_p^{(c)}(0) = 0$  (Ref. 26). When an excess density of pairs,  $p^{(0)}$ , is produced in a semi-infinite specimen (for example, by illumination or ionization by collision<sup>23</sup>), the density throughout the interior of the specimen is  $p^{(0)}$  in the absence of heating. There is, however, a

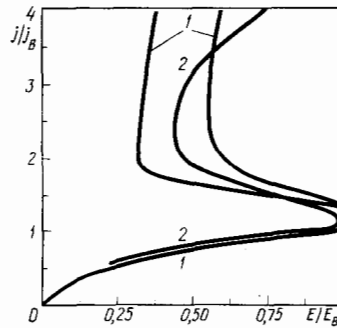


FIG. 15. Current-voltage characteristics for anomalous collection, recorded between a pair of probes separated by 0.44 mm from one another near the cathode. The material was n-InSb at 77 K. The plasma was produced by collisional ionization ( $E_B$  is the threshold field). 1—Calculation<sup>27</sup>; 2—experiment.<sup>23</sup> The descending branch of the characteristic is the result of the increase in the plasma density between the probes due to anomalous collection.

narrow region near the cathode (of the order of the diffusion length  $l_D = \sqrt{D\tau}$ ), where  $\Gamma_D^{(c)}$  falls to zero and the density rises sharply. In the presence of heating, a long ( $\sim l_E$ ) region of high plasma density may appear near the cathode.<sup>26</sup> This phenomenon is called anomalous collection and was observed in Ref. 23. The current-voltage characteristics are then of the S-shaped form (Fig. 15). When  $p^{(0)} < N_D$  and  $\Gamma_p(p^{(0)}) > \Gamma_p(p_h)$ , the plasma density rises discontinuously from  $p^{(0)}$  to  $p_2$  as the cathode is approached (the region 3  $\rightarrow$  4 in Fig. 13), and then smoothly increases from  $p_2$  to  $p_h$  with the scale  $\sim l_E$ . Thus,  $p(0) = p_h$  in the drift approximation. Immediately next to the cathode, there is a narrow diffusion region in which the plasma density is high and the flux falls to zero. For  $N_D < p^{(0)} < p_h$ , the density rises smoothly from  $p^{(0)}$  to  $p_h$  over a length of the order of  $l_E$ , and the shock is absent from the interior of the specimen.

The injection of holes into a finite n-InSb specimen was investigated in Ref. 24 at 77 K with  $p^{(0)} = 0$  and a collecting back contact. The boundary conditions were  $p^{(0)} = \infty$ ,  $\Gamma_p^{(c)}(L) = 0$ , where  $L$  is the length of the specimen. Depending on the current and length (or, more precisely, on the ratio  $L/L_h$ , where  $L_h = b_p E_h \tau$ ), very different density profiles can occur in the interior of the specimen,<sup>27</sup> consisting of segments of drift solutions and diffusion shocks (Fig. 16). Since the thickness of the latter is negligible, it follows from (6.4) that

$$\sum \int V(p) \frac{dp}{R(p, p^{(0)})} = L, \quad (6.5)$$

where the sum is evaluated over segments corresponding to drift solutions. This equation, together with the evolution condition, enables us to construct unambiguously the density distribution in the specimen. The value of  $L/L_h$  under the conditions of the experiment reported in Ref. 24 was 1.3.

The current-voltage characteristic is shown in Fig. 17 for this case. The S-shaped curve is due to anomalous collection.

Direct determination of the density profile with the simultaneous inclusion of drift, diffusion, and recombination is an exceedingly difficult problem. It is solved in Refs. 46 and 47 for a number of cases. It then turns out that the den-

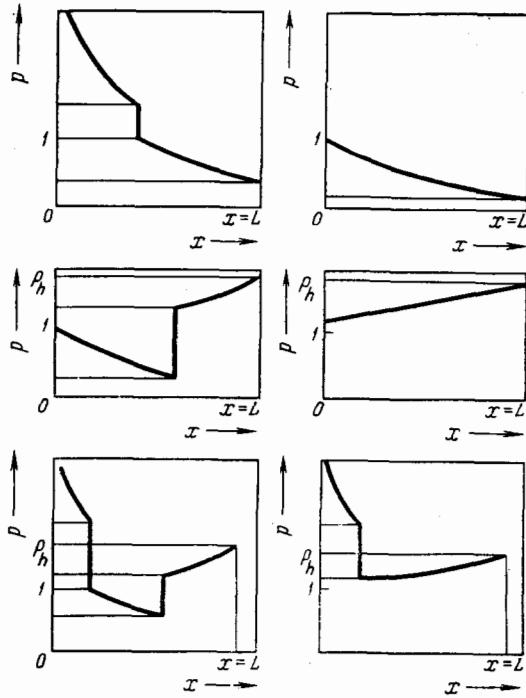


FIG. 16. Plasma density profiles in a specimen of finite length. The concentration  $p$  is in units of  $N_D$ .

sity profiles consist of steep and smooth segments corresponding to diffusion shocks (in the contact region) and drift solutions. The basic results reported in Refs. 46 and 47 can therefore be readily obtained by the method described above.

The authors of Refs. 46 and 47 investigated the phenomena in a finite n-type specimen, using the weak carrier heating approximation. A short ( $L \ll L_h$ ) n-type specimen ( $p^{(0)} < N_D$ ) with an injecting anode and a collecting cathode was examined in Ref. 46. It was found that the density of

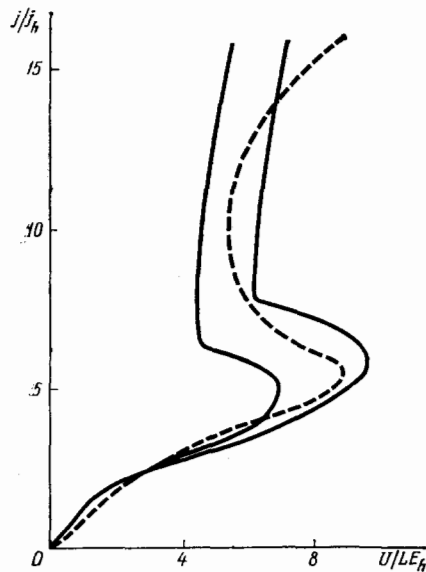


FIG. 17. Current-voltage characteristic of an n-InSb specimen of finite length. Solid line—calculated:  $L/L_h = 1$  for the left-hand line and  $L/L_h = 1.5$  for the right-hand line. Broken curve is experimental<sup>24</sup>;  $E_h = 15$  V/cm;  $L/L_h = 1.3$ .

holes on the boundary of the diffusion region near the cathode, given by

$$\int_{p(j;L)}^{\infty} \frac{dpV(j,p)}{R(p,p^{(0)})} = L, \quad (6.5')$$

was greater than  $N_D$  at all points. The injection shock was not therefore formed, and cold injection occurred everywhere for high currents ( $p > p_h$ ). For currents  $j = j' > 2j_h$ , determined by  $p(j',L) = p_h$ , a shock appeared at the cathode "above the well." It moved into the specimen as the current increased, and separated the region of cold injection from the region of anomalous collection. When  $j = j'' > 4j_h$ , the shock reached the anode, and the injection segment vanished. The magnitude of  $j''$  was determined from

$$\int_{p(j'',0)}^{p_h} \frac{V(j'',p)}{R(p,p^{(0)})} dp = L, \quad \Gamma_p(p(j'',0)) = \Gamma_0.$$

The authors of Ref. 47 examined a specimen with  $p^{(0)} \gg n^{(0)} - p^{(0)} = N_D$  and perfect ohmic contact ( $S$  is a contact with infinite recombination rate). On injection, it was the cathode and, on collection, the anode. In the case of injection (into the  $p^+$ -n-S-structure), the length  $l_E$  into which the carriers were injected increased with increasing current, and the dependence of the current on voltage was  $j \sim U^2$  (Ref. 9). When the current is high enough, the graph of  $\Gamma_p(p)$  shows the presence of a "well." For example, when  $L$  is less than the length corresponding to the injection drift region  $(\infty, p_k)$ , where  $p_k$  satisfies the equation  $\Gamma_p(p_k) = \Gamma_p(p^{(0)})$ , the density decreases smoothly from  $p = \infty$  to  $p = p(j,L)$  (6.5'), and falls rapidly at the cathode to  $p^{(0)}$ . As the current increases,  $\Gamma_p(p^{(0)})$  increases more rapidly than  $\Gamma_p(p_k)$ . Hence, the length of the segment  $(\infty, p_k)$  decreases and becomes smaller than  $L$ . At the same time, the injection drift segment continues to  $p = p_k$ , and thereafter the density falls discontinuously to  $p^{(0)}$ . Elsewhere in the specimen,  $p = p^{(0)}$  right up to the cathode. As the current increases further, the shock  $p_k \rightarrow p^{(0)}$  reaches the anode. At this point,  $p = p^{(0)}$  throughout the specimen, as for low currents; the current-voltage characteristic reaches the sublinear law (Fig. 18).

In the case of the collecting cathode (S-n-n<sup>+</sup>-structure), the density in a sufficiently long specimen is determined for  $j > 2j_h$  by anomalous collection, and changes from  $p = p(j,0)$  to  $p = p_h$  where  $p(j,0)$  is given by

$$\int_{p(j,0)}^{p_h} \frac{V(p)}{R(p,p^{(0)})} dp = L.$$

As the current increases,  $p(j,0)$  approaches  $p_h$ , and the field approaches  $E_h$ , so that the voltage across the specimen tends to  $E_h L$ .

### C. Shocks in a semiconductor with carriers captured by traps<sup>21</sup>

Real semiconductors frequently contain impurities that produce deep levels in the forbidden band. They act as carrier traps. In general, the situation is quite complicated. However, if the trapping times are very different, and the current is high enough, the profile again consists of drift

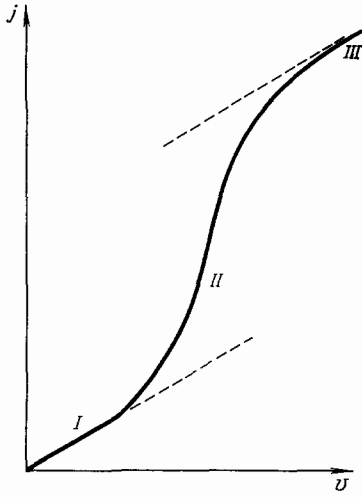


FIG. 18. Current-voltage characteristic of a  $p^+-n$ -S-structure for low values of  $L$  (Ref. 47). Segments I, III correspond to  $p = p_2^{(0)}$ ; segment II corresponds to injection;  $j \sim U^2$ .

segments and sharp shocks. Suppose, for example, that the specimen contains not only shallow fully ionized donors, but also  $N_t$  traps. The hole trapping time and the interband recombination time will be assumed to be long in comparison with all the characteristic times of the problem, and the electron trapping time  $\tau_n$  will be assumed to be small. In the drift approximation we then have the following equation for the holes:

$$\frac{\partial p}{\partial t} + \frac{\partial \Gamma_p}{\partial x} = \frac{\partial p}{\partial t} + \frac{\partial}{\partial x} (b_p p E) = 0 \quad (6.6)$$

and for the electrons:

$$\frac{\partial n}{\partial t} + \frac{\partial \Gamma_n}{\partial x} = \frac{\partial n}{\partial t} - \frac{\partial}{\partial x} (b_n n E) = [(n + n_t) f - n] \tau_n^{-1}, \quad (6.7)$$

where  $f$  is the degree of filling of the traps and the remaining notation is standard.<sup>48</sup>

When the density profile is sufficiently smooth ( $L \gg b_n E \tau_n$ ), the electrons are in equilibrium with traps, so that it follows from (6.7) that

$$f = \tilde{f} = \frac{n}{n + n_t}. \quad (6.8)$$

Substituting (6.8) into the quasistationarity condition

$$n = p + N_t (f_0 - f), \quad f_0 = 1 + \frac{N_D}{N_t}, \quad (6.9)$$

we obtain the relation between  $p$  and  $n$ :

$$p = n - N_t \left( f_0 - \frac{n}{n + n_t} \right). \quad (6.10)$$

Eliminating the electric field from the system (6.6)–(6.7), we obtain

$$\frac{\partial p}{\partial t} + V(p) \frac{\partial p}{\partial x} = 0, \quad V(p) = \frac{j b_n b_p (n - p) \frac{dn}{dp}}{e (b_n n + b_p p)^2} = \frac{d\Gamma_p}{dp}. \quad (6.11)$$

According to (6.10),  $d\Gamma_p/dp > 0$ ,  $d^2\Gamma_p/dp^2 < 0$  (Fig. 19). Evolution and breaking of the density profile occur, in this case, essentially as described in Section 2A. The structure of the shock is, however, more complicated.

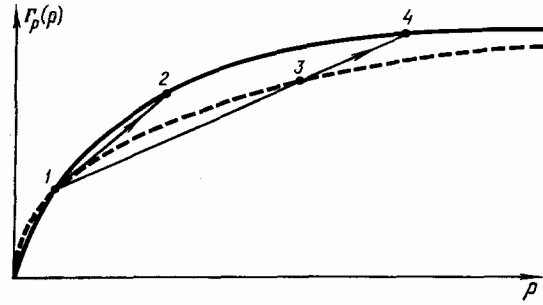


FIG. 19. Drift flux of holes in a semiconductor containing traps. Broken curve—drift flux at constant level of filling of traps corresponding to point 1.

#### D. Structure of a shock in a specimen containing traps. Relaxation zone

The degree of filling of traps undergoes a change in a shock. The characteristic time for this process is  $\sim \tau_n$ . When  $l_n + W\tau_n \gg l_T$ , the problem is analogous to that of a shock wave propagating in a medium with relaxation (see Section 4C<sup>13-15</sup>).

For a moderate density gradient, the quantities within the shock vary relatively slowly on a scale  $\sim l_n$ . This type of shock is illustrated by the segment 1  $\rightarrow$  2 in Fig. 19. According to the evolution condition, the density must increase in the shock. Let us now transform to  $X = x - Wt$  in (6.6)–(6.7). Neglecting diffusion, we obtain

$$\frac{\partial}{\partial X} (-Wp + b_p p E) = 0, \quad (6.12)$$

$$\frac{\partial}{\partial X} (-Wn - b_n n E) = [(n + n_t) f - n] \tau_n^{-1}. \quad (6.13)$$

Eliminating the electric field from the last two equations and then integrating (6.12), we obtain the relation between  $n$  and  $p$  in the shock:

$$-Wp + \frac{b_p p j}{e (b_n n + b_p p)} = K, \quad (6.14)$$

$$W = \frac{\Gamma_p(p^+) - \Gamma_p(p^-)}{p^+ - p^-}, \quad K = \frac{\Gamma_p(p^-) p^+ - \Gamma_p(p^+) p^-}{p^+ - p^-}, \quad (6.15)$$

where  $p^+$ ,  $p^-$  are the hole densities on the boundaries of the shock. Since, according to (6.12),  $d\Gamma_p/dX + d\Gamma_n/dX = W dp/dX$ , we have instead of (6.13)

$$W \left( 1 - \frac{dn}{dp} \right) \frac{dp}{dX} = [(n + n_t) f - n] \tau_n^{-1} < 0, \quad (6.16)$$

where  $n$  and  $p$  are related by (6.14) and (6.15). When  $dn/dp > 1$ , equation (6.16) defines a monotonic density profile in a shock with a scale  $\sim l_n$ . The trap filling function is given by (6.9).

If the density gradient in the shock is high enough, the quantity  $(1 - dn/dp) = N_t df/dp$ , obtained by solving (6.16), changes sign. This means that a smooth profile with a scale  $l_n$  is impossible. In fact, the profile consists of the diffusion shock 1  $\rightarrow$  3 of Fig. 19 and the segment 3  $\rightarrow$  4 of the solution (6.16) with the scale  $l_n$  (Ref. 31). This region is analogous to the relaxation zone in a shock wave.

There is a large number of practically important situations that can be described in terms of the model in which, in

addition to shallow donors and traps, there is an acceptor level (compensator).<sup>10,48</sup> The dependence of the drift current on density may then be nonmonotonic because both mobile and stationary shocks are possible. The situation is, however, complicated by the fact that recombination instability sets in even for relatively low currents, when  $l_E \sim l_D \sim l_T$ , and beginning with which it is meaningful to introduce the subdivision into diffusion shocks and drift profiles. Recombination instability occurs.<sup>49</sup>

The development of instability must, of course, modify the nature of the profile. However, a sharp subdivision of the specimen into two regions with different plasma densities must remain. Experiments to observe recombination instability<sup>50</sup> have, in fact, shown the presence of well-defined separation of the specimen into two regions with high and low electric fields. Large-amplitude oscillations were observed in the high-field region in accordance with the criterion given in Ref. 49. It seems likely, therefore, that the position of the boundary between the regions did not coincide with the position of the shock predicted by the stationary theory.

## 7. CONCLUSION

The breaking of smooth profiles and the formation of shock waves (discontinuities in solutions of the truncated equations) are concepts that are widely used in the analysis of fast processes in plasmas. These include shock waves,<sup>15,51</sup> collisionless shock waves,<sup>32,52</sup> and formation of double layers.<sup>53,54</sup>

It is clear from the examples considered in this review that the steepening of drift profiles and the formation of sharp density shocks are also relatively general features of slow (as compared with acoustic and Alfvén velocities) processes in inhomogeneous current-carrying collisional plasmas. The approach based on the reduction of the order of the original set of equations (1.1)–(1.3), and on the reduction of these equations to the equations for simple nonlinear waves, turns out to be very effective and leads to a physically clear picture of the phenomena. In many cases, it enables us to obtain simple analytic solutions.

Such phenomena must play an important role in the physics of space and laboratory plasmas, as well as in the physics and technology of gas discharges, semiconductors, and electrolytes. There has been relatively little experimental work in which such shocks have been unambiguously recorded, and there are practically no studies of their structure. It is therefore desirable to initiate detailed experimental studies of both shock formation and shock structure. In particular, since the density gradient in shocks is high, a variety of instabilities can develop in such shocks in the first instance. It is therefore essential to identify the conditions under which the shock structure is determined by classical processes and those under which it is governed by turbulence.

The authors are indebted to V. I. Perel' for stimulating discussions.

<sup>11</sup>When  $k = 3$  and one of the mobilities is zero, the velocity of the corresponding signals is referred to in semiconductor physics as the velocity of ambipolar drift.<sup>10</sup> Its measurements are widely used to investigate transport in semiconductors.<sup>11,12</sup>

<sup>2</sup>When the current  $j$  flowing through the plasma depends on time, we can, by replacing the time with the variable  $i$ , i.e., the charge passing through the plasma,<sup>16,17</sup> reduce the equation to (2.3).

$$q = \int_0^t j(t') dt'$$

<sup>3</sup>This case occurs, for example, in an  $n$ -type semiconductor with fully ionized donors of density  $n_2^{(0)}$ .

<sup>4</sup>A rigorous mathematical analysis of this type of quasilinear equation with a small parameter in front of the highest-order derivative is given in Ref. 33.

<sup>5</sup>The width of this shock is  $\sim l_T$ . Its structure is relatively difficult to determine because  $l_T$  is the electron energy relaxation length. On this scale, there is no local relationship between  $b_n$  and  $E$  (6.1) (Ref. 26). Even when it is possible to introduce the electron temperature, thermal diffusion and electron thermal conductivity must be taken into account over such lengths. On the other hand, in materials with inelastic scattering mechanisms (in particular, InSb), the length  $l_T$  is comparable with the mean free path, and a transport analysis is essential. However, the position and velocity of the shocks do not depend on the structure details.

<sup>1</sup>W. Schottky, Phys. Z. **25**, 342 (1924).

<sup>2</sup>H. Sabadil, Beitr. Plasmaphys. **13**, 235 (1973).

<sup>3</sup>M. Scholer and G. Haerendel, Planet. Space Sci. **19**, 915 (1971).

<sup>4</sup>A. P. Zhilinskii and L. D. Tsendin, Usp. Fiz. Nauk **131**, 343 (1980) [Sov. Phys. Usp. **23**, 331 (1980)].

<sup>5</sup>A. V. Nedospasov and V. D. Khait, Kolebaniya i neustoičivosti nizkotemperaturnoi plazmy (Oscillations and Instabilities of Low-Temperature Plasmas), Nauka, Moscow, 1979.

<sup>6</sup>L. Pekarek, Usp. Fiz. Nauk **94**, 463 (1968) [Sov. Phys. Usp. **11**, 188 (1968)].

<sup>7</sup>A. V. Eletskiĭ and A. T. Rakhimov, V kn. Khimiya plazmy (in: Plasma Chemistry), ed. by B. M. Smirnov, Atomizdat, Moscow, 1977, No. 4, p. 123.

<sup>8</sup>A. P. Napartovich and A. N. Starostin, V kn. Khimiya Plazmy (in: Plasma Chemistry), ed. by B. M. Smirnov, Atomizdat, Moscow, 1979, No. 6, 153.

<sup>9</sup>M. A. Lampert and P. Mark, Current Injections in Solids, Academic Press, 1970 (Russ. transl., Mir, M., 1973).

<sup>10</sup>V. L. Bonch-Bruевич and S. G. Kalashnikov, Fizika poluprovodnikov (Physics of Semiconductors), Nauka, M., 1977, Chap. 7.

<sup>11</sup>W. Shockley and J. Haynes, Phys. Rev. **81**, 835 (1951).

<sup>12</sup>A. C. Prior, Proc. Phys. Soc. London **76**, 465 (1960).

<sup>13</sup>G. B. Whitham, Linear and Nonlinear Waves, Wiley, 1974 [Russ. transl., Mir, Moscow, 1977].

<sup>14</sup>L. D. Landau and E. M. Lifshitz, Mekhanika sploshnykh sred, Fizmatgiz, M., 1954, [Engl. transl. Fluid Mechanics, Pergamon Press, Oxford, 1959].

<sup>15</sup>Ya. B. Zel'dovich and Yu. P. Raizer, Fizika udarnykh voln i vysokotemperaturnykh gazodinamicheskikh yavlenii (Physics of Shock Waves and High-Temperature Gas-Dynamic Phenomena), Nauka, M., 1966, [Engl. transl. of Ch. I only, elements of Gas Dynamics and the Classical Theory of Shock Waves, Academic Press, N. Y. 1968].

<sup>16</sup>F. Kolrausch, Ann. Phys. Chem. **62**, 209 (1897).

<sup>17</sup>H. Weber, Sitz. Akad. Wiss. Berlin **44**, 936 (1897).

<sup>18</sup>M. von Laue, Z. Anorg. Chem. **93**, 329 (1915).

<sup>19</sup>E. R. Smith, Bureau Stand. J. Res. **6**, 917 (1931).

<sup>20</sup>A. G. Longworth, J. Am. Chem. Soc. **65**, 1755 (1943).

<sup>21</sup>A. M. Stefanovskii, Author's Abstract of Thesis for Candidate's Degree, Leningrad Physicotechnical Institute, 1950.

<sup>22</sup>A. V. Gurevich, Pis'ma Zh. Eksp. Teor. Fiz. **8**, 193 (1968) [JETP Lett. **8**, 115 (1968)].

<sup>23</sup>S. Tosima, J. Phys. Soc. Jpn. **20**, 1814 (1965).

<sup>24</sup>S. Tosima and K. Ando, *ibid.* **23**, 812 (1967).

<sup>25</sup>A. P. Dmitriev, A. E. Stefanovich, and L. D. Tsendin, Fiz. Tekh. Poluprovodn. **9**, 1358 (1975) [Sov. Phys. Semicond. **9**, 894 (1975)].

<sup>26</sup>A. E. Stefanovich and L. D. Tsendin, Fiz. Tekh. Poluprovodn. **10**, 682 (1976) [Sov. Phys. Semicond. **10**, 406 (1976)].

<sup>27</sup>A. P. Dmitriev, A. E. Stephanovich, and L. D. Tsendin, Phys. Status Solidi **A 46**, 45 (1978).

<sup>28</sup>A. J. Scannapieco, S. L. Ossakow, D. L. Book, B. E. McDonald, and S. R. Goldman, J. Geophys. Res. **79**, 2913 (1974).

<sup>29</sup>V. A. Rozhanskii and L. D. Tsendin, Geomagn. Aeronom. **24**, 414 (1984).

<sup>30</sup>V. A. Rozhanskii and L. D. Tsendin, *ibid.* **598**.



- <sup>31</sup>A. P. Dmitriev and L. D. Tsendin, *Fiz. Tekh. Poluprovodn.* **19**, 2025 (1985) [sic].
- <sup>32</sup>*Elektrodinamika plazmy (Plasma Electrodynamics)*, ed. by A. I. Akhiezer, Nauka, Moscow, 1974, p. 107.
- <sup>33</sup>I. M. Gel'fand and Z. Ya. Shapiro, *Usp. Mat. Nauk* **14**, 87 (1959).
- <sup>34</sup>V. L. Granovskii, *Elektricheskiĭ tok v gaze. Ustanovivshisya tok (Electrical Current in Gases. Steady-State Current)*, Nauka, Moscow, 1971, p. 450.
- <sup>35</sup>Yu. S. Akishev, S. V. Dvurechenskii, A. P. Napartovich, S. V. Pashkin, and N. I. Trushkin, *Teplofiz. Vys. Temp.* **20**, 30 (1982).
- <sup>36</sup>Yu. S. Akishev, F. I. Vysikaĭlo, A. P. Napartovich, and V. V. Ponomarenko, *Teplofiz. Vys. Temp.* **18**, 266 (1980).
- <sup>37</sup>K. H. Lloyd and G. Haerendel, *J. Geophys. Res.* **78**, 7389 (1973).
- <sup>38</sup>N. I. Dzubenko *et al.*, *Planet. Space Sci.* **31**, 849 (1983).
- <sup>39</sup>I. S. Ivchenko, V. A. Rozhanskii, Yu. Ya. Ruzhin, V. S. Skomarovskii, and L. D. Tsendin, Preprint IZMIRAN, No. 6(417), Troitsk, 1983.
- <sup>40</sup>N. I. Zabusky, J. H. Doles III, and F. W. Perkins, *J. Geophys. Res.* **78**, 711 (1973).
- <sup>41</sup>V. A. Rozhanskii, *Fiz. Plazmy* **7**, 745 (1981) [*Sov. J. Plasma Phys.* **7**, 406 (1981)].
- <sup>42</sup>A. V. Gurevich and E. E. Tsedilina, *Usp. Fiz. Nauk* **91**, 609 (1967) [*Sov. Phys. Usp.* **10**, 214 (1967)].
- <sup>43</sup>G. Veittsner, V. kn. *Osnovy fiziki plazmy (in: Fundamentals of Plasma Physics)*, ed. by A. A. Galeev and R. Sudan, Energoatomizdat, Moscow, 1983, Vol. 1, p. 201.
- <sup>44</sup>H. Grad, *Rev. Mod. Phys.* **32**, 830 (1960).
- <sup>45</sup>S. Fornaca, *Phys. Fluids* **26**, 797 (1983).
- <sup>46</sup>A. A. Akopyan and Z. S. Gribnikov, *Solid-State Electron.* **19**, 41 (1976).
- <sup>47</sup>A. A. Akopyan and Z. S. Gribnikov, *Fiz. Tekh. Poluprovodn.* **9**, 1485 (1975) [*Sov. Phys. Semicond.* **9**, 981 (1975)].
- <sup>48</sup>J. S. Blakemore, *Semiconductor Statistics*, Pergamon, Oxford, 1962 [Russ. Transl., Mir, M., 1964].
- <sup>49</sup>O. V. Konstantinov and V. I. Perel', *Fiz. Tverd. Tela (Leningrad)* **6**, 3364 (1964) [*Sov. Phys. Solid State* **6**, 2691 (1965)].
- <sup>50</sup>I. V. Karpova, S. G. Kalashnikov, O. V. Constantinov, V. I. Perel, and G. V. Tsarenkov, *Phys. Status Solidi* **33**, 863 (1969).
- <sup>51</sup>A. C. Kolb and R. H. Griem, in: *Atomic and Molecular Processes*, ed. by D. Bates, Academic Press, New York, 1962 [Russ. Transl. in *Usp. Fiz. Nauk* **82**, 83 (1964)].
- <sup>52</sup>R. Z. Sagdeev, V. kn. *Voprosy teorii plazmy (in: Problems in Plasma Theory)*, ed. by M. A. Leontovich, Atomizdat, M. 1964, No. 4, p. 20, [Engl. Transl. *Reviews of Plasma Physics*, Consultants Bureau, N. Y., 1966].
- <sup>53</sup>H. Alfvén, *Cosmic Plasma*, Reidel, 1981 [Russ. Transl., Mir, M., 1983].
- <sup>54</sup>V. A. Liperovskii and M. I. Pudovkin, *Anomal'noe soprotivlenie i dvoĭnye sloi v magnitosfernoi plazme (Anomalous Resistance and Double Layers in Magnetospheric Plasma)*, Nauka, M., 1983.
- <sup>55</sup>F. I. Vysikaĭlo, *Fiz. Plazmy* **11**, 2215 (1985) [sic].

Translated by S. Chomet